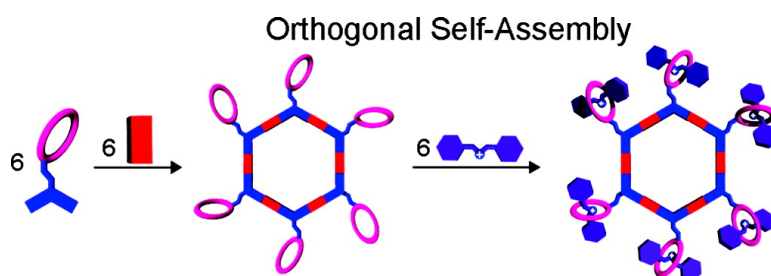Article

Coordination-Driven Self-Assembly of Cavity-Cored Multiple Crown Ether Derivatives and Poly[2]pseudorotaxanes

Koushik Ghosh, Hai-Bo Yang, Brian H. Northrop, Matthew M. Lyndon, Yao-Rong Zheng, David C. Muddiman, and Peter J. Stang

Orthogonal Self-Assembly

More About This Article

Additional resources and features associated with this article are available within the HTML version:

- Supporting Information
- Links to the 3 articles that cite this article, as of the time of this article download
- Access to high resolution figures
- Links to articles and content related to this article
- Copyright permission to reproduce figures and/or text from this article

View the Full Text HTML

Coordination-Driven Self-Assembly of Cavity-Cored Multiple Crown Ether Derivatives and Poly[2]pseudorotaxanes

Koushik Ghosh,[†] Hai-Bo Yang,*,[†] Brian H. Northrop,[†] Matthew M. Lyndon,[§]
Yao-Rong Zheng,[†] David C. Muddiman,[§] and Peter J. Stang*,[†]

*Departments of Chemistry, University of Utah, 315 South 1400 East, Room 2020, Salt Lake City,
Utah 84112, and North Carolina State University, Raleigh, North Carolina 27695*

Received December 31, 2007; E-mail: hbyang@chem.utah.edu; stang@chem.utah.edu

Abstract: The synthesis of a new 120° diplatinum(II) acceptor unit and the self-assembly of a series of two-dimensional metallacyclic polypseudorotaxanes that utilize both metal–ligand and crown ether−dialkyl-ammonium noncovalent interactions are described. Judiciously combining complementary diplatinum(II) acceptors with bispyridyl donor building blocks, with an acceptor and/or donor possessing a pendant dibenzo[24]crown-8 (**DB24C8**) moiety, allows for the formation of three new rhomboidal bis-**DB24C8**, one new hexagonal tris-**DB24C8**, and four new hexakis-**DB24C8** metallacyclic polygons in quantitative yields. The size and shape of each assembly, as well as the location and stoichiometry of the **DB24C8** macrocycle, can be precisely controlled. Each polygon is able to complex two, three, or six dibenzylammonium ions without disrupting the underlying metallacyclic polygons, thus producing eight different poly[2]pseudorotaxanes and demonstrating the utility and scope of this orthogonal self-assembly technique. The assemblies are characterized with one-dimensional multinuclear (^{1}H and ^{31}P) and two-dimensional ([1]H−^{1}H COSY and NOESY) NMR spectroscopy as well as mass spectrometry (ESI-MS). Further analysis of the size and shape of each assembly is obtained through molecular force-field simulations. ^{1}H NMR titration experiments are used to establish thermodynamic binding constants and poly[2]pseudorotaxane/dibenzylammonium stoichiometries. Factors influencing the efficiency of poly[2]pseudorotaxane formation are discussed.

The use of noncovalent interactions in modern synthetic chemistry allows for the selective and spontaneous formation, through the dynamic self-assembly of reversible yet robust linkages, of stable, highly complex supramolecular structures with specific functionalities, architectures, topologies, and/or properties.[1] One of the chief motivating factors for exploring supramolecular chemistry is the desire to synthesize new robust, functional, and technologically important materials. Many examples[2] from nature have demonstrated the power of self-assembly in constructing biologically relevant materials in which the self-assembled whole is greater than the sum of its parts. In biological ensembles such as collagen and enzymes,[3] for example, the combination of the individual molecular components is not solely responsible for their unique properties. Rather, their unique properties depend heavily on the specific spatial orientations of multicomponent structures that result from natural self-assembly and molecular organization. With the aim of obtaining a deeper understanding of the nature of such biological processes, a great deal of effort has been put forth to investigate artificial functional supramolecular systems.[4] Although the promise and potential of supramolecules that are obtained through accurately controlling chemical structure and functionality at the macromolecular level is considerable, it should be realized that this is not a simple process given the distinctive features of macromolecules compared to small molecules (e.g., number of functional groups, molecular weight distribution, purification techniques, etc.). Therefore, the elucidation of nanoscale molecular synthetic protocols that proceed with structural fidelity and a high level of functional group compatibility remains a great challenge.

Coordination-driven self-assembly has proven to be a highly efficient strategy for the construction of discrete two-dimensional (2-D) and three-dimensional (3-D) architectures with well-

[†] University of Utah.
[§] North Carolina State University.

(1) (a) Lehn, J.-M. *Angew. Chem., Int. Ed.* **1990**, *29*, 1304. (b) Philip, D.; Stoddart, J. F. *Angew. Chem., Int. Ed.* **1996**, *35*, 1155. (c) Whitesides, G. M.; Grzybowski, B. *Science* **2002**, *295*, 2418. (d) Lehn, J. M. *Proc. Natl. Acad. Sci. U.S.A.* **2002**, *99*, 4763. (e) Hori, A.; Yamashita, K.-I.; Fujita, M. *Angew. Chem., Int. Ed.* **2004**, *43*, 5016.
(2) (a) Kushner, D. J. *Bacteriol Rev.* **1969**, *33*, 302. (b) Gellman, S. H. *Chem. Rev.* **1997**, *97*, 1231. (c) Neidle, S. *Oxford Handbook of Nucleic Acid Structure*; Oxford University Press: Oxford, 1999. (d) Jones, M. N.; Chapman, D. *Micelles, Monolayers, and Biomembranes*; Wiley-Liss: New York, 1995. (e) Kauffman, S. *At Home in the Universe: the Search for Laws of Self Organization and Complexity*; Oxford University Press: New York, 1995.
(3) (a) Horne, R. W. *Virus Structure*; Academic Press: New York, 1974. (b) Groll, M.; Dizel, L.; Löwe, J.; Stock, D.; Bochter, M.; Bartunik, H. D.; Huber, R. *Nature* **1997**, *386*, 463.

(4) (a) Ikkala, O.; Brinke, G. *Science* **2002**, *295*, 2407. (b) Fiedler, D.; Bergman, R. G.; Raymond, K. N. *Angew. Chem., Int. Ed.* **2006**, *45*, 745. (c) Pluth, M. D.; Bergman, R. G.; Raymond, K. N. *Science* **2007**, *316*, 85. (d) Yoshizawa, M.; Tamura, M.; Fujita, M. *Science* **2006**, *312*, 251. (e) Nishioka, Y.; Yamaguchi, T.; Yoshizawa, M.; Fujita, M. *J. Am. Chem. Soc.* **2007**, *129*, 7000. (f) Leung, D. H.; Bergman, R. G.; Raymond, K. N. *J. Am. Chem. Soc.* **2007**, *129*, 2746. (g) Qin, L.; Banholzer, M. J.; Xu, X.; Huang, L.; Mirkin, C. A. *J. Am. Chem. Soc.* **2007**, *129*, 14870. (h) Masar, M. S., III; Gianneschi, N. C.; Oliveri, C. G.; Stern, C. L.; Nguyen, S. T.; Mirkin, C. A. *J. Am. Chem. Soc.* **2007**, *129*, 10149. (i) Gianneschi, N. C.; Bertin, P. A.; Nguyen, S. T.; Mirkin, C. A.; Zakharov, L. N.; Rheingold, A. L. *J. Am. Chem. Soc.* **2003**, *125*, 10508.

defined shapes and sizes.[5] However, many of the ensembles prepared to date have been built from simple, fairly inert building blocks that are often aliphatic or aromatic in nature. Stimulated by the possibility of constructing artificial functional nanoscale devices with predesigned shapes and sizes, recent efforts have focused on incorporating functionality into the final discrete assemblies.[6,7] For example, we have previously reported the facile synthesis of snowflake-shaped metallodendrimers with hexagonal cavities as their cores.[6c] Fujita and co-workers have prepared saccharide-coated $M_{12}L_{24}$ molecular spheres that form aggregates through multiple interactions with proteins.[7e] Encouraged by the power and versatility of coordination-driven self-assembly in the design and synthesis of novel supramolecular species with desired functionality, we envisioned that the specific control over chemical structure and functionality at the macromolecular level can be realized by employing the coordination-driven strategy and can allow for the formation of more complicated multiple functional architectures, such as multiple crown ether derivatives and higher-order pseudorotaxanes.

Since first introduced by Pedersen in 1967,[8] crown ethers and their structural analogues have attracted significant attention from various fields of science, as can be illustrated by numerous literature reports of their applications in host–guest chemistry and the construction of structurally interesting molecular architectures.[9] During the past two decades, considerable research interest has been devoted to the design of multiple crown ether derivatives, which can be used in multicomponent host–guest recognition or in the construction of higher-order complexes.[10] However, considering the time-consuming procedures and low yields generally achieved by traditional covalent synthetic strategies, noncovalent synthetic methodologies may provide a new path for the formation of such sophisticated compounds.
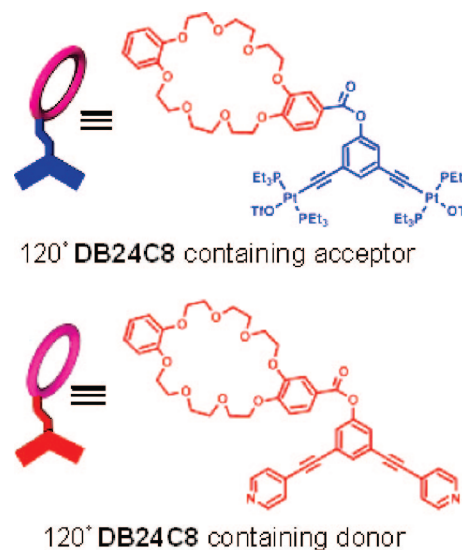

Figure 1. Molecular structures of 120° **DB24C8**-containing acceptor and 120° **DB24C8**-containing donor.

In addition, crown ethers, along with other macrocycles such as cyclodextrins, cucurbiturils, and tetracationic cyclobis(paraquat-*p*-phenylene) cyclophanes, have been extensively used for the construction of rotaxanes and pseudorotaxanes.[11] As a consequence of their structural properties and potential applications as nanoscale devices, chemists have been inspired to prepare novel interwoven architectures based upon polyrotaxanes and polypseudorotaxanes.[12] Nevertheless, systematic investigations of the synthesis of polypseudorotaxanes, especially higher-order polypseudorotaxanes, are still rare.

As indicated above, the incorporation of functionality into well-defined 2-D and 3-D ensembles can be achieved by coordination-driven self-assembly.[6,7] More importantly, this methodology allows for precise control over each parameter of composition, structure, and overall macromolecular topology. We have previously reported a highly efficient approach to prepare tris(dibenzo[24]crown-8) derivatives and hexagonal cavity-cored tris[2]pseudorotaxanes.[6d] Herein, we present a much extended investigation of the self-assembly of different sized and shaped multiple crown ether derivatives and poly[2]pseudorotaxanes, from bis[2]pseudorotaxanes up to hexakis[2]pseudorotaxanes, thus demonstrating the wide-ranging efficiency and applicability of this approach.

A new novel dibenzo[24]crown-8 (**DB24C8**)-containing 120° di-Pt(II) acceptor building block has been designed and prepared. A series of different sized and shaped multiple crown ether derivatives can be formed in nearly quantitative yield when this new 120° **DB24C8** di-Pt(II) acceptor and/or the known 120° **DB24C8** dipyridyl donor[6d] (Figure 1) are combined with different complementary angle precursors (donors or acceptors) via coordination-driven self-assembly in one single step. A reasonable extension of these strategies is the utilization of

(5) (a) Stang, P. J.; Olenyuk, B. *Acc. Chem. Res.* **1997**, *30*, 502. (b) Leininger, S.; Olenyuk, B.; Stang, P. J. *Chem. Rev.* **2000**, *100*, 853. (c) Seidel, S. R.; Stang, P. J. *Acc. Chem. Res.* **2002**, *35*, 972. (d) Schwab, P. F. H.; Levin, M. D.; Michl, J. *Chem. Rev.* **1999**, *99*, 1863. (e) Holliday, B. J.; Mirkin, C. A. *Angew. Chem., Int. Ed.* **2001**, *40*, 2022. (f) Cotton, F. A.; Lin, C.; Murillo, C. A. *Acc. Chem. Res.* **2001**, *34*, 759. (g) Fujita, M.; Tominaga, M.; Hori, A.; Therrien, B. *Acc. Chem. Res.* **2005**, *38*, 369. (h) Fiedler, D.; Leung, D. H.; Bergman, R. G.; Raymond, K. N. *Acc. Chem. Res.* **2005**, *38*, 349. (i) Gianneschi, N. C.; Masar, M. S., III.; Mirkin, C. A. *Acc. Chem. Res.* **2005**, *38*, 825.

(6) (a) Yang, H.-B.; Das, N.; Huang, F.; Hawkridge, A. M.; Diaz, D. D.; Arif, A. M.; Finn, M. G.; Muddiman, D. C.; Stang, P. J. *J. Org. Chem.* **2006**, *71*, 6644. (b) Yang, H.-B.; Das, N.; Huang, F.; Hawkridge, A. M.; Muddiman, D. C.; Stang, P. J. *J. Am. Chem. Soc.* **2006**, *128*, 10014. (c) Yang, H.-B.; Hawkridge, A. M.; Huang, S. D.; Das, N.; Bunge, S. D.; Muddiman, D. C.; Stang, P. J. *J. Am. Chem. Soc.* **2007**, *129*, 2120. (d) Yang, H.-B.; Ghosh, K.; Northrop, B. H.; Zheng, Y.-R.; Lyndon, M. M.; Muddiman, D. C.; Stang, P. J. *J. Am. Chem. Soc.* **2007**, *129*, 14187. (e) Yang, H.-B.; Ghosh, K.; Zhao, Y.; Northrop, B. H.; Lyndon, M. M.; Muddiman, D. C.; White, H. S.; Stang, P. J. *J. Am. Chem. Soc.* **2008**, *130*, 839.

(7) (a) Merlau, M. L.; Del Pilar Mejia, M.; Nguyen, S. T.; Hupp, J. T. *Angew. Chem., Int. Ed.* **2001**, *40*, 4239. (b) Sun, S.-S.; Stern, C. L.; Nguyen, S. T.; Hupp, J. T. *J. Am. Chem. Soc.* **2004**, *126*, 6314. (c) Murase, T.; Sato, S.; Fujita, M. *Angew. Chem., Int. Ed.* **2007**, *46*, 1083. (d) Kawano, M.; Kawamichi, T.; Haneda, T.; Kojima, T.; Fujita, M. *J. Am. Chem. Soc.* **2007**, *129*, 15418. (e) Kamiya, N.; Tominaga, M.; Sato, S.; Fujita, M. *J. Am. Chem. Soc.* **2007**, *129*, 3816.

(8) Pedersen, C. J. *J. Am. Chem. Soc.* **1967**, *89*, 7017.

(9) For recent reviews on crown ether and its analogues, see: (a) Bradshaw, J. S.; Izatt, R. M. *Acc. Chem. Res.* **1997**, *30*, 338. (b) Gokel, G. W.; Leevy, W. M.; Weber, M. E. *Chem. Rev.* **2004**, *104*, 2723. (c) Jarosz, S.; Listkowski, A. *Curr. Org. Chem.* **2006**, *10*, 643. (d) Steed, J. W. *Coord. Chem. Rev.* **2001**, *215*, 171. (e) Ritch, J. S.; Chivers, T. *Angew. Chem., Int. Ed.* **2007**, *46*, 4610. (f) Tsukube, H. *Coord. Chem. Rev.* **1996**, *148*, 1.

(10) (a) Sasaki, S.; Shionoya, M.; Koga, K. *J. Am. Chem. Soc.* **1985**, *107*, 3371. (b) Voyer, N. *J. Am. Chem. Soc.* **1991**, *113*, 1818. (c) Voyer, N.; Roby, J.; Deschenes, D.; Bernier, J. *Supramol. Chem.* **1995**, *5*, 61. (d) Huang, Z. B.; Chang, S. H. *Synlett* **2005**, *14*, 2257. (e) Tanaka, M.; Higuchi, Y.; Adachi, N.; Shibutani, Y.; Ahmed, S. A.; Kado, S.; Nakamura, M.; Kimura, K. *Tetrahedron* **2005**, *61*, 8159. (f) Dykes, G. M.; Smith, D. K. *Tetrahedron* **2003**, *59*, 3999. (g) Sathiyendiran, M.; Liao, R.-T.; Thanasekaran, P.; Luo, T.-T.; Venkataramanan, N. S.; Lee, G.-H.; Peng, S.-M.; Lu, K.-L. *Inorg. Chem.* **2006**, *45*, 10052. (h) Li, C.; Law, G-L.; Wong, W.-T. *Org. Lett.* **2004**, *6*, 4841.

Scheme 1. Retrosynthetic Analysis of Multiple Crown Ether Derivatives with Cavities of Varying Size and Shape
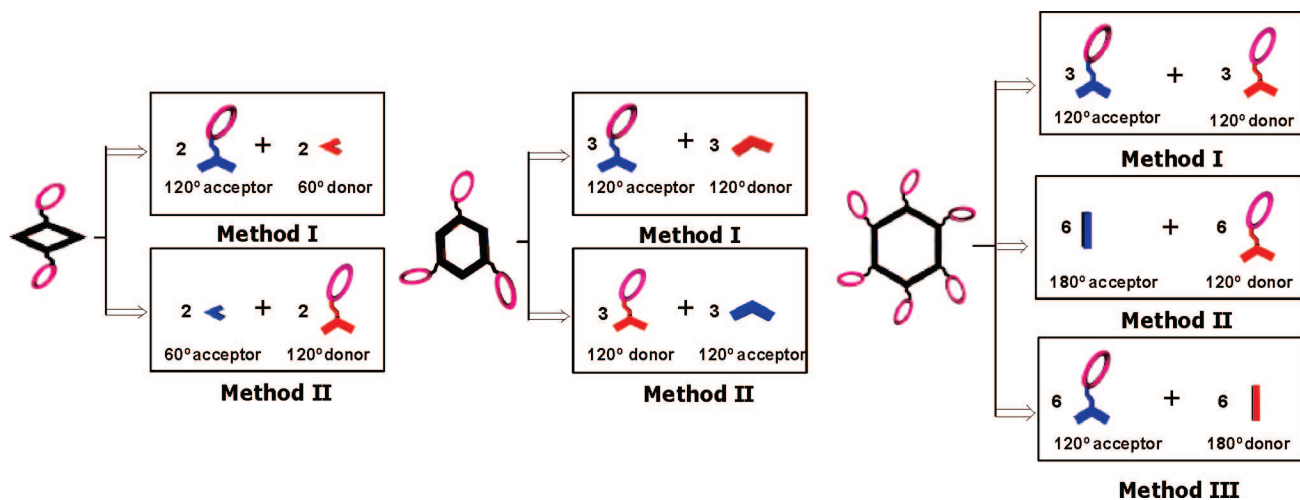
multiple crown ethers to incorporate dialkylammonium ions ($R_2NH_2^+$) for the formation of poly[2]pseudorotaxanes. By employing the non-interfering, orthogonal nature[13] of weak hydrogen bonding and electrostatic forces and relatively strong metal–ligand coordination bonding, a series of poly[2]pseudorotaxanes with well-designed shapes and different sized cavities was obtained. It is worth noting that, to the best of our knowledge, this is the first report of the formation of discrete hexakis-**DB24C8** derivatives and hexakis[2]pesudorotaxanes, which further enriches the library of higher-order supramolecular host–guest architectures.

Results and Discussion

Retrosynthetic Analysis of Polygonal Multiple Crown Ether Derivatives. According to the "directional bonding" model and the "symmetry interaction" model,[5] the shape of an

individual 2-D polygon is usually determined by the value of the turning angle within its angular components. For example, the combination of 60° units with complementary 120° linking components will yield a molecular rhomboid. Planar hexagonal structures can be self-assembled in two different ways based on the above-mentioned models. Discrete hexagonal entities of type $A^2_6L^2_6$ can be self-assembled from a combination of six shape-defining and directing corner units A_2 (containing two coordination sites which enclose a 120° angle) with six appropriate linear linker units L_2 (containing two coordination sites oriented 180° from each other). An alternative route for the assembly of hexagonal supramolecular systems involves the combination of two complementary ditopic building blocks, A^2 and X^2, each incorporating 120° angles between the active coordination sites, allowing for the formation of hexagonal structures of type $A^2_3X^2_3$.[5a]

By synthesizing a diverse library of donor and acceptor building blocks, two complementary strategies have been devised in order to construct "isomeric" supramolecular structures possessing the same geometry, though the turning angle of component donor and acceptor building blocks has been reversed. An example of such self-assembled structures can be found in the synthesis of cuboctahedra,[14a] where a pair of matching cages was assembled from two complementary sets of angular and tritopic building units. Similar reasoning has been applied in other nanoscopic cages, such as truncated tetrahedra and supramolecular M3L2prisms.[14b,c]

Complementary self-assembly strategies that utilize crown ether-derivatized 120° donors and/or 120° acceptors are explored herein to prepare bis-, tris-, and hexakis-**DB24C8** derivatives in one single step. Retrosynthetically, the concept used to prepare multiple crown ether-derivitized molecular polygons is summarized in Scheme 1. This coordination-driven self-assembly strategy for introducing crown ether moieties on the periphery of molecular polygons not only provides a strategy that can be built upon to devise additional routes to functionalized molecular polygons but also allows for a direct comparison of the properties of the multiple crown ether structures obtained from complementary units.

(11) (a) *Catenanes, Rotaxanes, and Knots*; Schill, G., Ed.; Academic Press: New York, 1971. (b) *Molecular Catenanes, Rotaxanes and Knots*; Dietrich-Buchecker, C. O., Sauvage, J. P., Eds.; Wiley-VCH: New York, 1999. (c) Sauvage, J. P. *Acc. Chem. Res.* **1990**, *23*, 319. (d) Hoss, R.; Vögtle, F. *Angew. Chem., Int. Ed.* **1994**, *33*, 375. (e) Amabilino, D. B.; Stoddart, J. F. *Chem. Rev.* **1995**, *95*, 2725. (f) Jäger, R.; Vögtle, F. *Angew. Chem., Int. Ed.* **1997**, *36*, 930. (g) Nepogodiev, S. A.; Stoddart, J. F. *Chem. Rev.* **1998**, *98*, 1959. (h) Sauvage, J. P. *Acc. Chem. Res.* **1998**, *31*, 611. (i) Raymo, F. M.; Stoddart, J. F. *Chem. Rev.* **1999**, *99*, 1643. (j) Tian, H.; Wang, Q.-C. *Chem. Soc. Rev.* **2006**, *35*, 361. (k) Wenz, G.; Han, B.-H.; Mueller, A. *Chem. Rev.* **2006**, *106*, 782. (l) Loethen, S.; Kim, J.-M.; Thompson, D. H. *Polym. Rev.* **2007**, *47*, 383.

(12) (a) Liu, Y.; Yu, L.; Chen, Y.; Zhao, Y.-L.; Yang, H. *J. Am. Chem. Soc.* **2007**, *129*, 10656. (b) Park, C.; Oh, K.; Lee, S. C.; Kim, C. *Angew. Chem., Int. Ed.* **2007**, *46*, 1455. (c) Hoffart, D. J.; Loeb, S. J. *Angew. Chem., Int. Ed.* **2005**, *44*, 901. (d) Huang, F.; Nagvekar, D. S.; Slebodnick, C.; Gibson, H. W. *J. Am. Chem. Soc.* **2005**, *127*, 484. (e) Lo Nostro, P.; Lopes, J. R.; Cardelli, C. *Langmuir* **2001**, *17*, 4610. (f) Yamaguchi, N.; Nagvekar, D. S.; Gibson, H. W. *Angew. Chem., Int. Ed.* **1998**, *37*, 2361. (g) Gibson, H. W.; Yamaguchi, N.; Jones, J. W. *J. Am. Chem. Soc.* **2003**, *125*, 3522. (h) ten Cate, A. T.; Kooijman, H.; Spek, A. L.; Sijbesma, R. P.; Meijer, E. W. *J. Am. Chem. Soc.* **2004**, *126*, 3801. (i) Yelamaggad, C. V.; Achalkumar, A. S.; Rao, D. S. S.; Prasad, S. K. *J. Am. Chem. Soc.* **2004**, *126*, 6506. (j) Kim, H. J.; Zin, W. C.; Lee, M. *J. Am. Chem. Soc.* **2004**, *126*, 7009.

(13) (a) Pollino, J. M.; Stubbs, L. P.; Weck, M. *Polym. Prepr.* **2003**, *44*, 730. (b) Pollino, J. M.; Stubbs, L. P.; Weck, M. *J. Am. Chem. Soc.* **2004**, *126*, 563. (c) Hofmeier, H.; El-ghayoury, A; Schenning, A. P. H. J.; Schubert, U. S. *Chem. Commun.* **2004**, 318. (d) Hofmeier, H.; Hoogenboom, R.; Wouters, M. E. L.; Schubert, U. S. *J. Am. Chem. Soc.* **2005**, *127*, 2913. (e) Kishore, R. S. K.; Paululat, T.; Schmittel, M. *Chem. Eur. J.* **2006**, *12*, 8136. (f) Kishore, R. S. K.; Kalsani, V.; Schmittel, M. *Chem. Commun.* **2006**, 3690.

(14) (a) Olenyuk, B.; Whiteford, J. A.; Fechtenkotter, A.; Stang, P. J. *Nature* **1999**, *398*, 796. (b) Kryschenko, Y. K.; Seidel, S. R.; Muddiman, D. C.; Nepomuceno, A. I.; Stang, P. J. *J. Am. Chem. Soc.* **2003**, *125*, 9647. (c) Leininger, S.; Fan, J.; Schmitz, M.; Stang, P. J. *Proc. Natl. Acad. Sci.* **2000**, *97*, 1380.

Scheme 2. Synthesis of 120° Angular Di-Pt(II) Acceptor Subunit **5**[a]
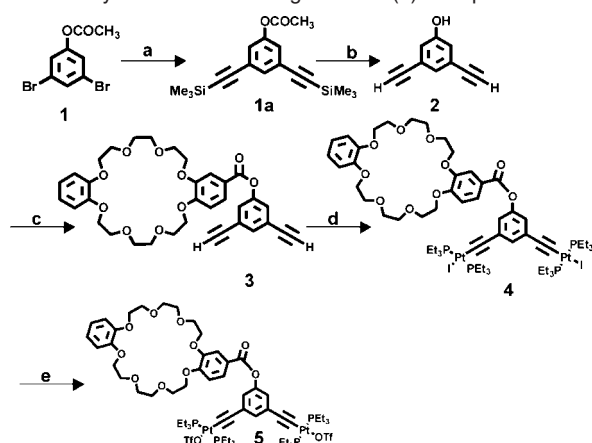
[a] Key: (a) (trimethylsilyl)acetylene, Pd(PPh₃)₄, CuI, Et₃N, THF, room temperature, 16 h (80%); (b) NaHCO₃, methanol/THF/water, reflux, 12 h (95%); (c) **DB24C8** carboxylic acid, DCC, DMAP, CH₂Cl₂, room temperature, 10 h (85%); (d) CuI, Et₂NH, toluene, room temperature, 16 h (65%); (e) AgOTf, CH₂Cl₂, room temperature, 4 h (90%).

Scheme 3. Two Complementary Ways To Self-Assemble Rhomboidal Bis-**DB24C8** Derivatives
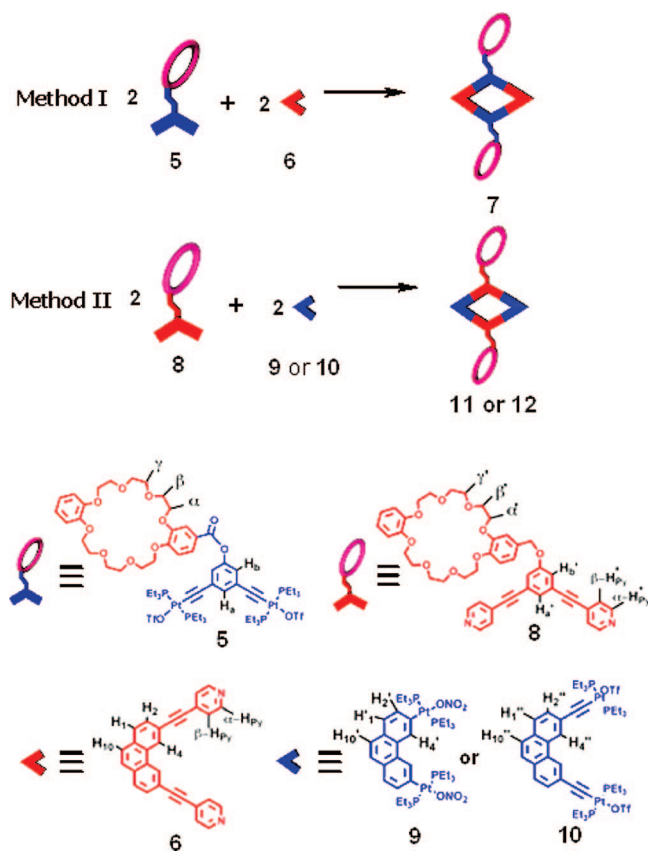
Synthesis of Angular 120° Crown Ether-Functionalized Acceptor Unit. The acidity of C−H bonds in alkynes induced by transition metals has received considerable attention in organometallic chemistry.[15] By taking advantage of the linear geometry of the alkynyl unit and its π-unsaturated character, the metal alkynyls have been extensively explored to prepare molecular wires and polymeric organometallic materials, which may possess interesting properties such as optical nonlinearity, luminescence, liquid crystallinity, and electrical conductivity.[16] Herein we utilize the coupling reaction of *trans*-PtI₂(PEt₃)₂ with
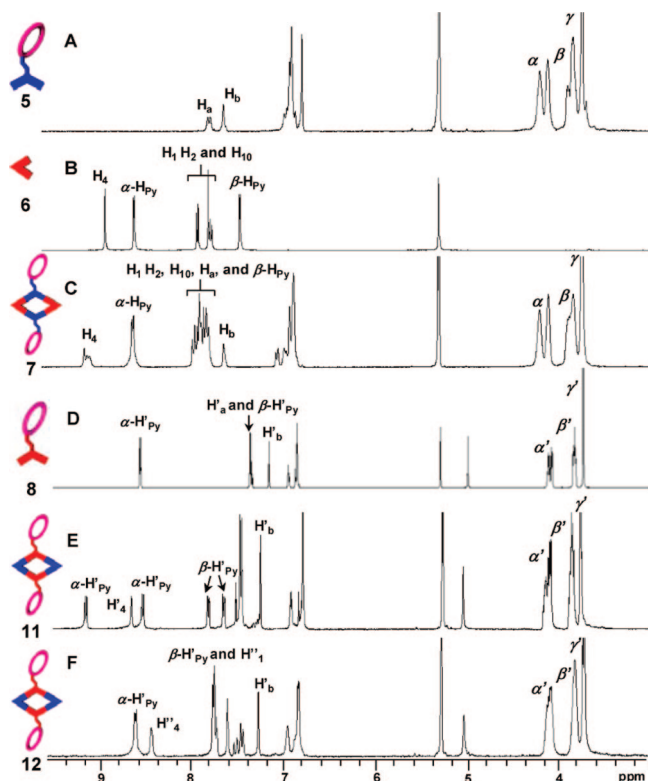

Figure 2. Partial ¹H NMR (500 MHz, CD₂Cl₂, 298 K) spectra of free building blocks **5** (A), **6** (B), and **8** (D) and rhomboids **7** (C), **11** (E), and **12** (F).

C−H bonds in alkynes as the key step to the synthesis of a novel 120° acceptor unit.

The 120° crown ether-containing di-Pt(II) acceptor **5** can be easily synthesized as indicated in Scheme 2. 3,5-Diethynyl-phenol (**2**) was prepared by palladium-mediated coupling of acetic acid 3,5-dibromo-phenyl ester (**1**) with (trimethyl-silyl)acetylene, followed by deprotection in a methanol/THF/water solvent mixture. The crown ether moiety was introduced by a coupling reaction of **2** with dibenzo[24]crown-8 carboxylic acid. Compound **3** was then reacted with 4 equiv of *trans*-PtI₂(Et₃)₂ to give diiodometal complex **4** in accordance with a similar procedure reported in the literature.[17] Subsequent halogen abstraction with AgOTf resulted in the isolation of bistriflate salt **5** in reasonable yield (38% overall). In the ³¹P NMR spectrum, the diplatinum acceptor **5** displayed a singlet at 22.7 ppm, accompanied by flanking ¹⁹⁵Pt satellites. Attempts to grow single crystals for X-ray diffraction studies of **5** failed; therefore,

(15) (a) Yang, H.-B.; Ghosh, K.; Arif, A. M.; Stang, P. J. *J. Org. Chem.* **2006**, *71*, 9464. (b) Yang, H.-B.; Ghosh, K.; Das, N.; Stang, P. J. *Org. Lett.* **2006**, *8*, 3991. (c) Werner, H.; Bachmann, P.; Martin, M. *Can. J. Chem.* **2001**, *79*, 519. (d) John, K. D.; Hopkins, M. D. *Chem. Commun.* **1999**, 589. (e) Werner, H.; Bachmann, P.; Laubender, M.; Gevert, O. *Eur. J. Inorg. Chem.* **1998**, 1217. (f) Wong, W.-Y.; Wong, C.-K.; Lu, G.-L.; Lee, A. W.-M.; Cheah, K.-W.; Shi, J.-X. *Macromolecules* **2003**, *36*, 983. (g) Berenguer, J. R.; Bernechea, M.; Fornies, J.; Lalinde, E.; Torroba, J. *Organometallics* **2005**, *24*, 431. (h) Vicente, J.; Chicote, M.-T.; Alvarez-Falcon, M. M.; Jones, P. G. *Organometallics* **2005**, *24*, 2764.

(16) (a) Paul, F.; Lapinte, C. *Coord. Chem. Rev.* **1998**, *178–180*, 431. (b) Ziessel, R.; Hissler, M.; El-ghayoury, A.; Harriman, A. *Coord. Chem. Rev.* **1998**, *178–180*, 1251. (c) Nguyen, P.; Gómez-Elipe, P.; Manners, I. *Chem. Rev.* **1999**, *99*, 1515. (d) Dembinski, R.; Bartik, T.; Bartik, B.; Jaeger, M.; Gladysz, J. A. *J. Am. Chem. Soc.* **2000**, *122*, 810. (e) Long, N. J.; Williams, C. K. *Angew. Chem., Int. Ed.* **2003**, *42*, 2586.

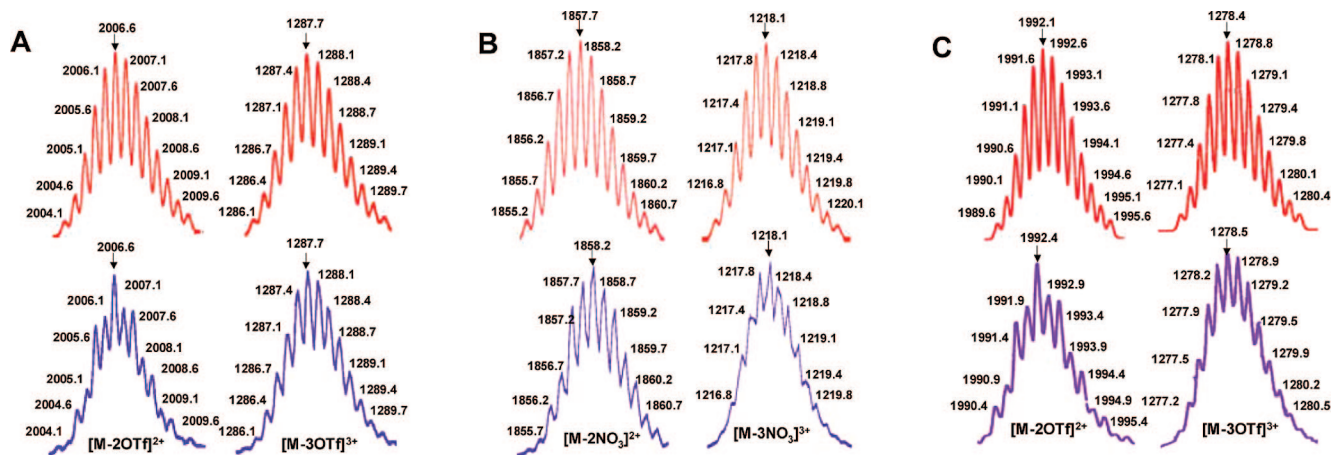(17) Leininger, S.; Stang, P. J.; Huang, S. *Organometallics* **1998**, *17*, 3981.

Figure 3. Calculated (top) and experimental (bottom) ESI-MS spectra of rhomboids **7** (A), **11** (B), and **12** (C).

the distance between the two platinum centers was estimated using molecular mechanics force-field (MMFF) simulations and shown to be ∼1.0 nm (see Supporting Information). It is worth noting that compound **5** is unique in the sense that it carries sites for multiple recognition: the crown ether can recognize cations or small organic compounds and the Pt(II) center can act as an acceptor unit to a variety of ligands.

Self-Assembly of Rhomboidal Bis-DB24C8 Derivatives. With the 120° crown ether-containing precursors—both donor and acceptor—in hand, the self-assembly of crown ether derivatives with rhomboidal cavities was investigated. As discussed above, the combination of 60° units with 120° linking components will yield a molecular rhomboid. Upon mixing the newly designed 120° acceptor unit **5** and the 60° donor **6** in dichloromethane, bis-**DB24C8** rhomboid **7** was obtained (Scheme 3, Method I). In a complementary manner (Scheme 3, Method II), stirring the crown ether-containing 120° angular donor **8** with an equimolar amount of the known 60° angular Pt(II) acceptor, 2,9-(*trans*-Pt(PEt$_3$)$_2$NO$_3$)$_2$-phenanthrene (**9**), in dichloromethane resulted in the rhomboidal structure **11**. By using different sized 60° angular Pt(II) acceptors, the size of the rhomboidal cavity in the final assemblies can be controlled. For example, stirring acceptor **10** with 120° donor unit **8** for 30 min in dichloromethane gave bis-**DB24C8** rhomboid **12**, which possesses a slightly larger rhomboidal cavity size compared to ensemble **11**. Molecular modeling studies show an inner cavity diameter of 1.6 nm for **11**, whereas the cavity diameter of **12** is 2.0 nm (see Supporting Information).

The self-assembly of rhomboids **7**, **11**, and **12** was monitored by multinuclear NMR spectroscopy. Analysis of the ^{31}P NMR spectrum of each reaction solution is consistent with the formation of highly symmetric species, by the appearance of a sharp singlet (16.0 ppm for **7**, 12.6 ppm for **11**, and 16.1 ppm for **12**, each with concomitant ^{195}Pt satellites), shifted by 6.7, 8.4, and 7.0 ppm upfield for **7**, **11**, and **12** relative to the signals for the starting acceptor units **6**, **9**, and **10**, respectively. Examination of the ^{1}H NMR spectra (Figure 2) also indicates the existence of highly symmetric structures. The ^{1}H NMR spectra display significant downfield shifts of the pyridyl proton signals (for α proton, Δδ = 0.02 ppm for **7**, 0.11 ppm for **11**, and 0.10 ppm for **12**; for β proton, Δδ = 0.41 ppm for **7**, 0.20 ppm for **11**, and 0.43 ppm for **12**), associated with the loss of electron density upon coordination by the nitrogen lone pair to platinum metal centers. An interesting dynamic effect was observed in rhomboid **7**, where the H$_4$ proton signals are found

Scheme 4. Two Complementary Ways To Self-Assemble Hexagonal Tris-**DB24C8** Derivatives
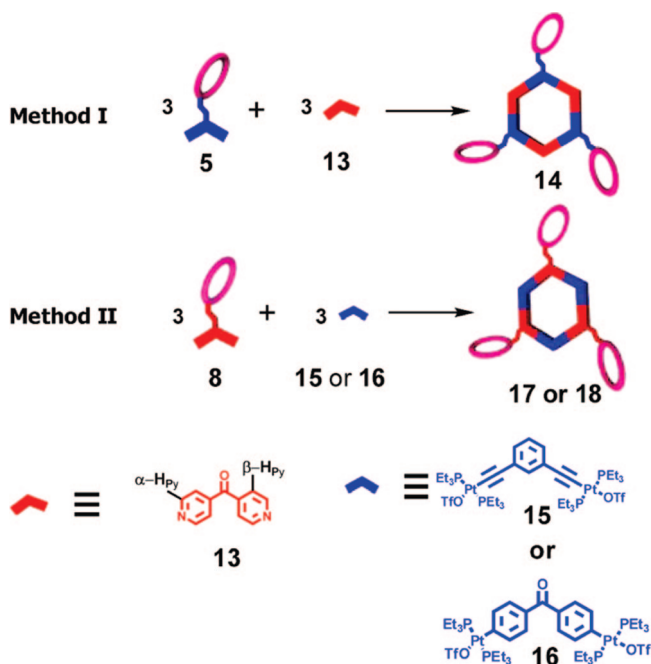
to be inequivalent, likely due to a slightly twisted structure resulting from the flexibility of the triple bonds in both acceptor and donor units. Moreover, in accordance with the previously reported molecular rectangles and trigonal bipyramidal cages, the inner and outer pyridyl protons of **11** are found to be inequivalent because of restricted rotation around the Pt—pyridine bond.[6a,14a,18]

Mass spectrometric studies of all three rhomboids were performed using the electrospray ionization mass spectral (ESI-MS) technique, which allows the assemblies to remain intact during the ionization process while obtaining the high resolution required for isotopic distribution. In the ESI-MS spectrum of rhomboid **7** (Figure 3A), for example, peaks attributable to the loss of triflate counterions, [M − 2OTf]$^{2+}$ (*m/z* = 2006.6) and [M − 3OTf]$^{3+}$ (*m/z* = 1287.7), where M represents the intact assembly, were observed and their isotopic resolutions are in excellent agreement with the theoretical distributions. Similarly,

(18) Tarkanyi, G.; Jude, H.; Palinkas, G.; Stang, P. J. *Org. Lett.* **2005**, *7*, 4971.
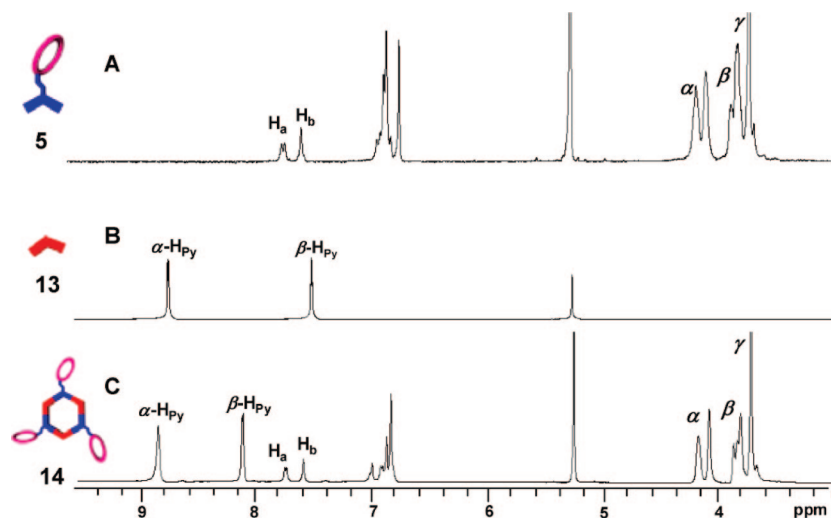
Figure 4. Partial ^{1}H NMR spectra of free building blocks **5** (A) and **13** (B) and hexagon **14** (C).
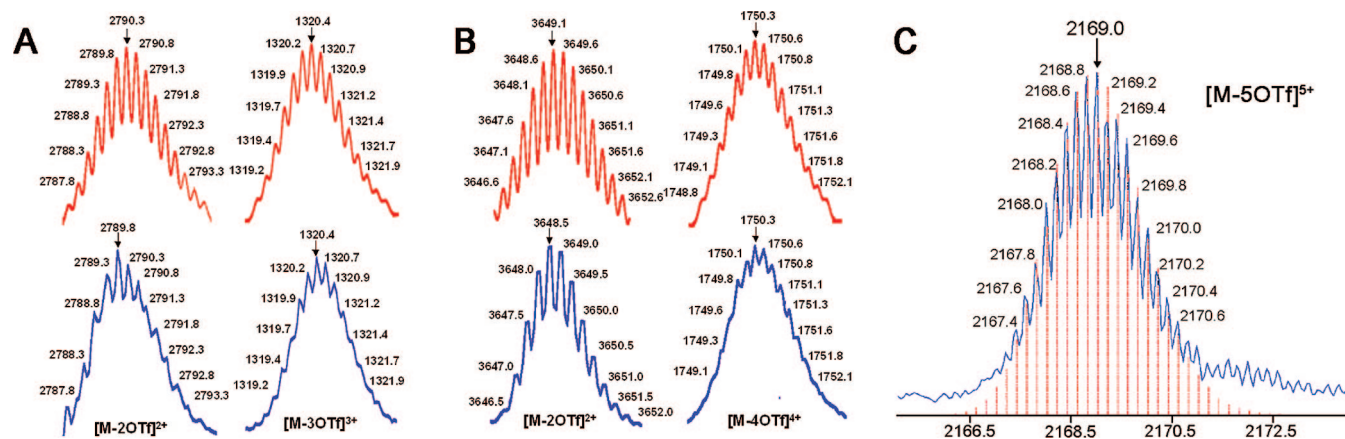

Figure 5. Calculated (top) and experimental (bottom) ESI-MS spectra of hexagonal tris-**DB24C8** derivative **14** (A) and hexagonal hexakis-**DB24C8** derivative **19** (B). ESI-TOF-MS spectrum of hexagonal hexakis-**DB24C8** derivative **25** (C). The vertical arrows are the theoretical abundances.

the ESI-MS spectra of rhomboids **11** and **12** (Figure 3B,C), exhibited two charged states at $m/z = 1857.7$ and $m/z = 1218.1$ for **11**, corresponding to $[M - 2NO_3]^{2+}$ and $[M - 3NO_3]^{3+}$, and at $m/z = 1992.1$ and $m/z = 1278.4$ for **12**, attributable to $[M - 2OTf]^{2+}$ and $[M - 3OTf]^{3+}$, respectively. These peaks were isotopically resolved, and they agree very well with their theoretical distribution.

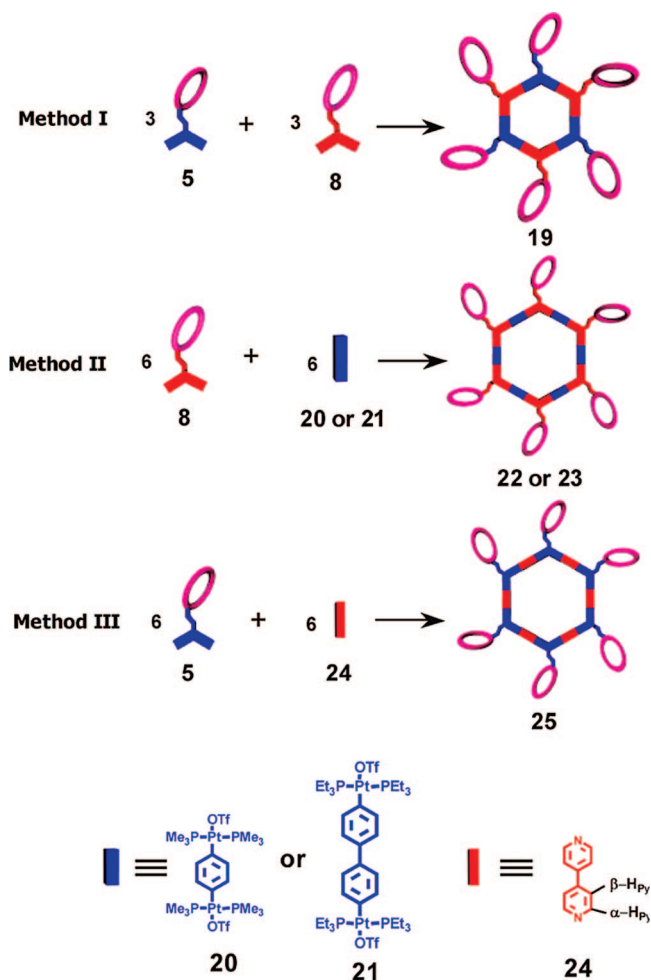**Self-Assembly of Hexgonal Tris-DB24C8 Derivatives.** Recently, in a preliminary communication, we have reported[6d] the self-assembly of tris-**DB24C8** derivatives with hexagonal cavities through the combination of the 120° **DB24C8**-derivatized donor subunit **8** with 120° di-Pt(II) acceptor **15** or **16** in a 1:1 stoichiometric ratio (Scheme 4, Method II). An extended investigation into the viability of preparing similar types of tris-**DB24C8** derivatives employing a complementary approach has now been undertaken. As shown in Scheme 4 (Method I), the hexagonal tris-**DB24C8** derivative **14** can also be easily synthesized by simply mixing the 120° **DB24C8**-containing acceptor subunit **5** and di-2-pyridyl ketone (**13**) in a 1:1 ratio in dichloromethane.

The ^{31}P NMR spectrum of **14** displayed a sharp singlet (ca. 16.0 ppm) shifted upfield from the signal for the starting platinum donor **5** by approximately 6.7 ppm, which suggests the formation of a discrete, highly symmetric assembly. This change, as well as the decrease in coupling of the flanking ^{195}Pt

satellites ($\Delta^1 J_{PPt} = -84.7$ Hz), is consistent with back-donation from complexed platinum atoms. In the ^{1}H NMR spectrum (Figure 4), the β protons displayed a dramatic downfield shift ($\Delta\delta = 0.65$ ppm) with respect to those of free donor **13** and the α protons shifted slightly as well ($\Delta\delta = 0.10$ ppm). ESI-MS spectrometry provides further evidence for the formation of the new hexagonal assembly **14**. In the mass spectrum of **14** (Figure 5A), peaks at $m/z = 2790.3$ and $m/z = 1320.4$, corresponding to $[M - 2 OTf]^{2+}$ and $[M - 3OTf]^{3+}$, respectively, were observed, and their isotopic resolutions are all in excellent agreement with their theoretical distributions. Molecular modeling studies reveal a smaller internal diameter of 2.3 nm for **14** as compared to 3.2 and 2.9 nm for **17** and **18**, respectively (see Supporting Information).

Self-Assembly of Hexgonal Hexakis-DB24C8 Derivatives. A more dramatic extension of functionalization by means of coordination-driven self-assembly is manifested in the construction of molecular hexagons with six crown ethers, where each crown ether moiety is on each of the vertices of the hexagon. As indicated in Scheme 5, six crown ethers can be introduced in molecular hexagons along three routes. The first method investigated utilizes three 120° donor units and three 120° acceptor units, each derivatized with one crown ether moiety, from which the [3+3] hexagon **19** can be self-assembled (Scheme 5, Method I).

180° linear 4,4′-bipyridyl donor **24** (Scheme 5, Method III), demonstrating a complementary method for the preparation of hexagonal hexakis-**DB24C8** assembly **25**. After 30 min of continuous stirring at room temperature, initial visual evidence of the completion of self-assembly processes was indicated by the complete dissolution of starting materials and formation of a homogeneous yellow solution. More quantitative evidence of successful self-assembly was then obtained from characteristic changes observed in each assembly's NMR spectra. In all three cases, the analysis of ^{31}P NMR spectra of the reaction solution is consistent with the formation of highly symmetric species, as indicated by the appearance of one sharp singlet (−14.8 ppm for **22**, 14.1 ppm for **23**, and 16.3 ppm for **25**) with concomitant ^{195}Pt satellites shifted upfield from the signals for their respective acceptor building blocks ($\Delta\delta = 8.5$ ppm for **22**, 8.1 ppm for **23**, and 6.4 ppm for **25**). As expected, a decrease in coupling of the flanking ^{195}Pt signals ($\Delta^1J_{PPt} = -130$ Hz for **22**, $\Delta^1J_{PPt} = -155$ Hz for **23**, and $\Delta^1J_{PPt} = -67$ Hz for **25**) was also observed. Examination of the ^1H NMR spectrum (Figure 6) of each assembly is also indicative of highly symmetric structures. Only one set of peaks in the final self-assembly, arising from donor and acceptor units, and significant downfield shifts of the pyridyl proton signals (for α proton, $\Delta\delta = 0.11$ ppm for **22**, 0.23 ppm for **23**, and 0.10 ppm for **25**; for β proton, $\Delta\delta = 0.36$ ppm for **22**, 0.43 ppm for **23**, and 0.93 ppm for **25**), associated with the loss of electron density on coordination of the nitrogen lone pair to the platinum metal center, support the efficient self-assembly of hexagons **22**, **23**, and **25**. The sharp nature of the peaks supports the formation of molecular hexagons with six crown ethers as opposed to the formation of oligomers, which would significantly broaden the proton signals.

Compared to the previous multiple crown ether derivatives (**7**, **11**, **12**, **14**, and **17**–**19**), it has proven more difficult to get strong mass signals for dodeca-cationic ensembles **22**, **23**, and **25**, on account of their larger molecular weight, even under the ESI-TOF-MS conditions. Hexagonal crown ether derivative **23**, as a representative example, has a molecular weight of 12411 Da ($C_{498}H_{672}N_{12}O_{90}P_{24}Pt_{12}S_{12}$). With considerable effort, the peak attributable to $[M - 5OTf]^{5+}$ ($m/z = 2167.6$) was observed (Figure 5C) for **25** in the ESI-TOF-MS spectrum, along with isotopically resolved peaks (i.e., direct charge state determination), allowing for the molecularity of the crown ether-derivatized hexagon to be unambiguously established. For assemblies **22** and **23**, a peak corresponding to $[M - 5OTf]^{5+}$ was also observed in each ESI-MS spectrum; however, neither peak could be isotopically well resolved because of the high molecular weight of assemblies **22** and **23** (see Supporting Information).

All attempts to grow X-ray-quality single crystals of the hexagonal hexakis-**DB24C8** derivatives have so far proven unsuccessful. Therefore, molecular force-field simulations were used to gain further insight into the structural characteristics of these assemblies (Figure 7, see also Supporting Information). A 1.0 ns molecular dynamics simulation (MMFF) was used to equilibrate each supramolecule, followed by energy minimization of the resulting structures to full convergence. Simulations reveal that the underlying hexagonal structures—"scaffolds"—all retain their planar and rigid geometries, even when derivatized with pendent crown ether units. Internal diameters of 3.0, 5.2, 6.2, and 4.5 nm for **19**, **22**, **23**, and **25**, respectively, were observed. The methods outlined in Scheme 4 provide not only three different means of installing six crown ether units onto the periphery of molecular hexagons but also a direct, unam-

Stirring a mixture of acceptor (**5**) and donor (**8**) precursors in a 1:1 ratio in dichloromethane for 45 min results in a homogeneous clear yellow-orange solution. The ^{31}P NMR spectrum of this solution displayed a sharp singlet (ca. 18.3 ppm) shifted upfield from the signal for the starting platinum acceptor **5** by approximately 4.4 ppm. Moreover, a decrease in coupling of the flanking ^{195}Pt satellites ($\Delta J \approx -65$ Hz) was observed. In the ^1H NMR spectrum (Figure 6C), the proton signals of the pyridine ring hydrogen atoms exhibited downfield shifts (ca. α-H_{Py}, 0.1 ppm; β-H_{Py}, 0.4 ppm) typically observed upon coordination with Pt(II) complexes. ESI-MS spectrometry provides further evidence for the formation of the new hexagonal assembly **19**. In the mass spectrum of **19**, peaks at $m/z = 3649.2$ and $m/z = 1750.3$, corresponding to $[M - 2 OTf]^{2+}$ and $[M - 4 OTf]^{4+}$, respectively were observed, and their isotopic resolutions are all in excellent agreement with their theoretical distributions (Figure 5B).

As indicated in the retrosynthetic analysis (Scheme 1), the synthesis of hexagonal hexakis-**DB24C8** assemblies can also be achieved according to two additional complementary protocols from the combination of six 180° building blocks and six 120° angular subunits. The self-assembly of crown ether-derivatized donor **8** with different sized 180° linear acceptors **21** and **22** (Scheme 5, Method II) was investigated in dichloromethane, leading to the formation of crown ether-derivatized hexagons **22** and **23**, respectively. Along similar lines, crown ether-derivatized acceptor **5** was combined in a 1:1 ratio with
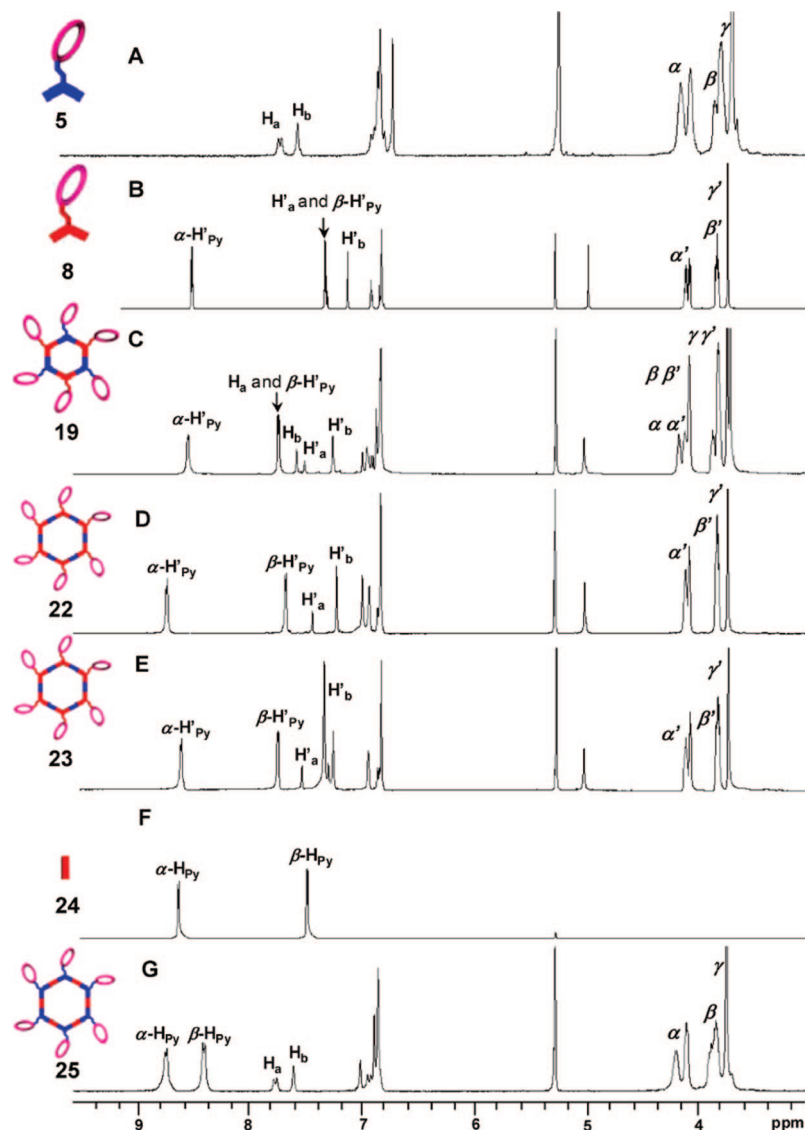
Figure 6. Partial ^{1}H NMR spectra (500 MHz, CD$_2$Cl$_2$, 298 K) of free building blocks **5** (A), **13** (B), and **24** (F) and hexagonal hexakis-**DB24C8** assemblies **19** (C), **22** (D), **23** (E), and **25** (G).
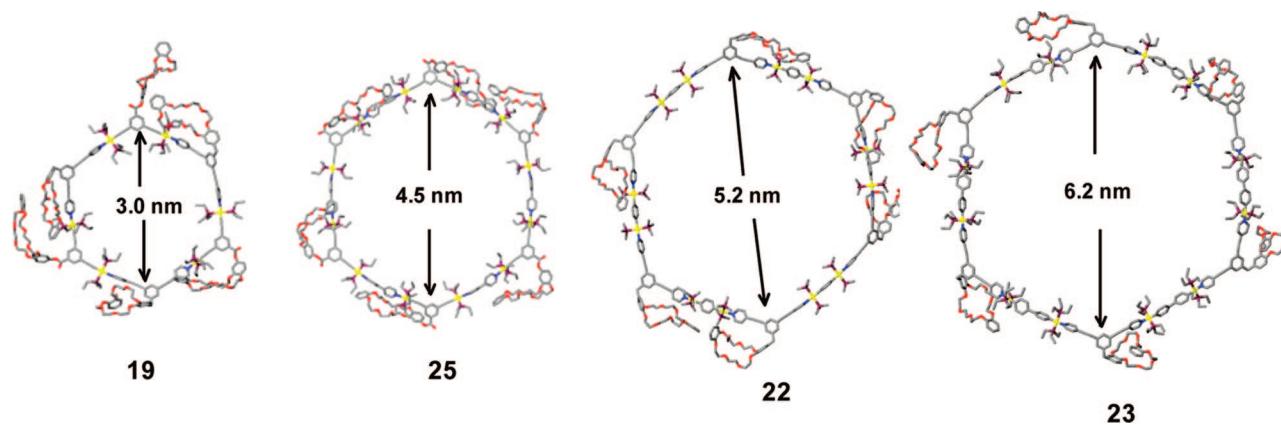

Figure 7. Simulated molecular model of hexagonal hexakis-**DB24C8** derivatives **19**, **25**, **22**, and **23**, optimized with the molecular mechanics force field. Color scheme: C, gray; O, red; N, blue; P, purple; and Pt, yellow (hydrogen atoms have been removed for clarity).

biguous means of varying the cavity size of these cavity-cored hexakis-crown ether derivatives while retaining the efficiency (i.e., short reaction time and high yield) of coordination-driven self-assembly. In all cases, the flexible nature of the pendent crown ether moieties and the rigid nature of the hexagonal cavity can be observed from modeling studies.

Scheme 6. Formation of Rhomboidal Cavity-Cored Bis[2]pseudorotaxanes

Scheme 7. Formation of Hexagonal Cavity-Cored Tris[2]pseudorotaxanes
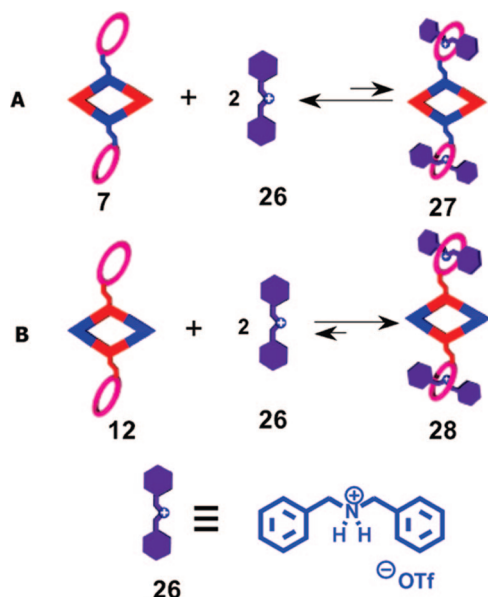
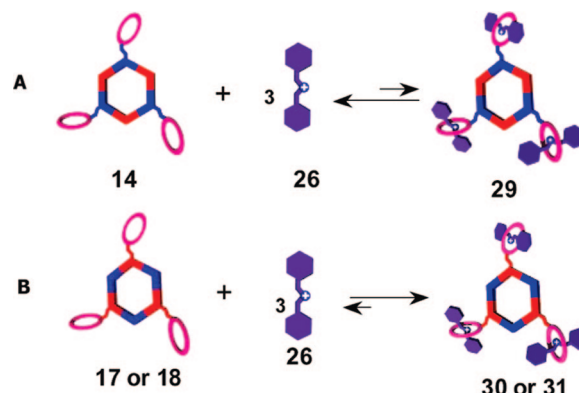All of the above collective analytical results indicate that multiple crown ether derivatives with predesigned shape and size can be easily prepared (>95% yields) through coordination-driven self-assembly, which avoids the time-consuming procedures and lower yields often encountered in covalent synthetic protocols. Previous approaches to the construction of single-molecule, non-polymeric multiple crown ether units have been limited to either the attachment of crown ethers to a helical peptide scaffold or dendritic construction of multiple crown ether units.[10] The approach outlined herein provides an alternative route to multiple crown ether molecules with different topologies and arrangements. Furthermore, the synthesis is straightforward and the yield is quantitative, which eliminates the need for purification. In particular, to the best of our knowledge, we have presented the first example wherein six crown ethers are uniquely and precisely positioned on the periphery of molecular polygons.

Investigation of the Self-Assembly of Poly[2]pseudorotaxanes. With these novel multiple crown ether derivatives in hand, an investigation of the self-assembly of poly[2]pseudorotaxanes was

carried out. For many years, crown ethers have been recognized as exceptionally versatile hosts for a wide variety of cationic guests, particularly for substituted ammonium ions. Although initial studies focused primarily upon alkylammonium ions[19] (RNH_3^+), more recently, secondary alkylammonium ions[20] ($R_2NH_2^+$) have received considerable attention. Numerous experimental investigations have demonstrated that appropriately sized crown ether macrocycles bind $R_2NH_2^+$ ions in solution, in the solid state, and in the gas phase in a threaded rather than face-to-face manner.[21] Consequent to these myriad studies, the high-affinity binding and molecular recognition motifs operative in the complexation between dialkylammonium ion centers ($-CH_2NH_2^+CH_2-$) and different crown ether macrocycles, e.g., **DB24C8**, are well established and understood. Mixing complementary host and guest components in a 1:1 molar ratio in low-polarity, nonprotic solvents (e.g., CH_2Cl_2, CH_3CN, etc.) results in the formation of a pseudorotaxane complex held by strong [N−H···O] hydrogen bonds between the acidic NH_2^+ protons and the oxygen atoms of the **DB24C8** ring. Additional [C−H···O] hydrogen-bonding and $\pi-\pi$ stacking interactions, as well as electrostatic forces, further contribute to the stability of the resultant pseudorotaxanes. By taking advantage of the complexation of dibenzylammonium ions ($C_6H_5CH_2NH_2^+CH_2-C_6H_5$) and **DB24C8** derivatives as well as the orthogonal, non-interacting nature of metal–ligand and hydrogen-bonding non-covalent interactions in solution, we envisioned that a new class of poly[2]pseudorotaxane complexes could be prepared from
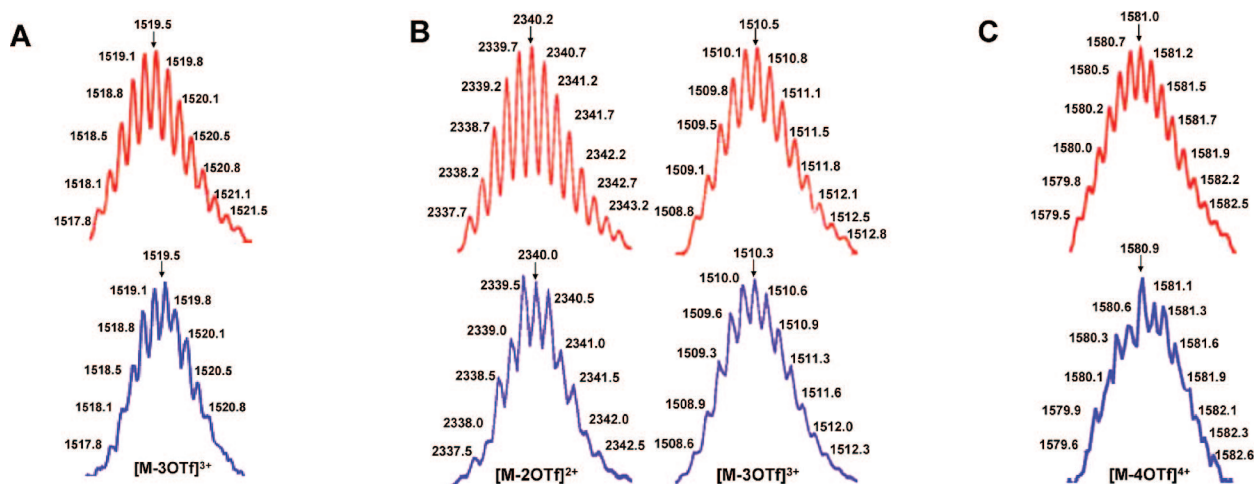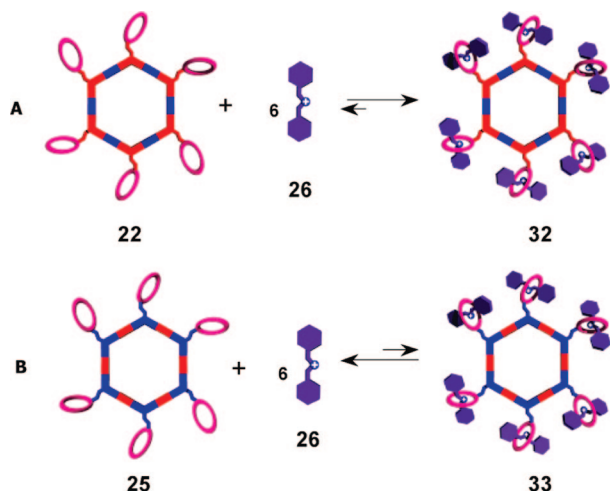

Figure 8. Calculated (top) and experimental (bottom) ESI-MS spectra of rhomboidal bis[2]pseudorotaxane **27** (A), rhomboidal bis[2]pseudorotaxane **28** (B), and hexagonal tris[2]pseudorotaxane **29** (C).

Scheme 8. Formation of Hexagonal Cavity-Cored Hexakis[6]pseudorotaxanes

molecular polygons functionalized with crown ether moieties on their periphery. The generation, by three different methods, of tris[2]pseudorotaxane structures via this orthogonal self-assembly strategy has been recently reported by our group.[6d] Herein we significantly expand upon these preliminary studies and demonstrate the formation of multiple different shaped and sized poly[2]pseudorotaxanes in a stepwise manner.

Within 15 min of adding 2 equiv of dibenzylammonium triflate salt **26** to a solution of rhomboidal bis-**DB24C8** derivatives **7** (2.25 mM) and **12** (2.33 mM) in dichloromethane, bis[2]pseudorotaxanes **27** and **28**, respectively, with rhomboidal cavities were obtained (Scheme 6). Compared to the spectra of free hosts **7** and **12**, the ^{31}P NMR spectrum of each complex does not exhibit any significant change, indicating that the threading process of dibenzylammonium ions does not substantially change the chemical environment of the phosphorus atoms present in the rhomboids. The ^{1}H NMR spectra of **27** and **28**, however, displayed characteristic shifts associated with the complexation of dibenzylammonium ion **26** by **DB24C8**. A 0.45 ppm downfield shift of the signal for the benzylic methylene protons adjacent to the NH_2^+ center

was observed in both spectra, and protons H_α, H_β, and H_γ of **DB24C8** exhibited upfield shifts of 0.03, 0.08, and 0.25 ppm, respectively. Further characterization with 2-D spectroscopic techniques ($^{1}H-^{1}H$ COSY and NOESY) are in agreement with the formation of the rhomboidal cavity-cored bis[2]pseudorotaxanes. For example, through-space interactions between the α-H proton of the complexed crown ether and the benzylic methylene protons were observed in the NOESY spectrum of each complex (see Supporting Information).

In the ^{1}H NMR spectrum of **28**, the formation of bis[2]pseudorotaxane as the prevailing product was supported by the observation of one dominant set of proton signals (>90% by integration) along with some signals for partially complexed and uncomplexed species at equilibrium. In the ^{1}H NMR spectrum of **27**, however, resonances attributable to uncomplexed glycol $-OCH_2CH_2O-$ protons of the crown ether rings and of free dibenzylammonium (**26**) were observed. The ratio of the complexed and uncomplexed species is approximately 1:1, as established by integration. This observation suggests that either (a) the kinetics of pseudorotaxane self-assembly is considerably slower for bis[2]pseudorotaxane **27** than for bis[2]pseudorotaxane **28** or (b) the binding constant of bis-**DB24C8** host **7** is lower than that of the related bis-macrocycle **12**. The first of these two possibilities is easily ruled out both intuitively (the kinetics of assembly should essentially be equal, given that derivatized macrocycles **7** and **12** have nearly identical size and structural characteristics) and experimentally (periodically checking the ^{1}H NMR spectrum of assembly **27** over several days revealed no changes, indicating that equilibrium had been reached). It is more likely that the electron-withdrawing effects of the proximal Pt(II) centers of the derivatized crown ether building block **5** decrease the binding ability of the crown ether sites of bis-host **7**, which in turn decrease the ratio of complexed to uncomplexed species to 1:1 at equilibrium.

Further quantitative proof of the existence of rhomboidal cavity-cored bis[2]pseudorotaxanes **27** and **28** is provided by ESI-MS spectrometry. A peak at $m/z = 1519.5$ was observed, corresponding to $[M - 3OTf]^{3+}$ for **27**, as were peaks attributable to $[M - 2OTf]^{2+}$ and $[M - 3OTf]^{3+}$ of **28** at $m/z = 2340.0$ and $m/z = 1510.3$, respectively. All peaks were isotopically resolved, and they agree very well with their theoretical distribution (Figure 8).

Hexagonal tris-**DB24C8** derivatives **17** and **18** can be used to prepare hexagonal tris[2]pseudorotaxanes **30** and **31** along three different routes by the orthogonal self-assembly strategy, as reported previously.[6d] New tris[2]pseudorotaxane **29**, which exhibits an architecture similar to those of **30** and **31**, has been obtained from the self-assembly of **14** and **26** in a 1:3 ratio (Scheme 7). The crown ether moieties of tris-host **14** are directly attached to di-Pt(II) acceptor building blocks rather than bispyridyl donor building blocks as in **17** and **18**, changing the electronic environment of host **14**. In the case of assembly **29**, the equilibrium ratio of complexed to uncomplexed species was observed to be somewhat less than 1:1, indicating a slight excess of uncomplexed species. This observation is analogous to the comparison of rhomboid bis[2]pseudorotaxanes **27** and **28** and further supports the conclusion that covalent attachment of the crown ether derivatives to di-Pt(II) acceptors lowers the binding abilities of the typically electron-rich macrocycles. Despite this shift in equilibrium, positive assignment of tris[2]pseudorotaxane **29** was obtained through ESI-MS, which revealed a peak at $m/z = 1580.9$, corresponding to $[M - 4OTf]^{4+}$. Two-dimensional spectroscopic techniques ($^{1}H-^{1}H$ COSY and

(19) (a) Cram, D. J.; Cram, J. M. *Science* **1974**, *183*, 803. (b) Cram, D. J.; Cram, J. M. *Acc. Chem. Res.* **1978**, *11*, 8. (c) Jong, F. D.; Reinhoudt, D. N. *Adv. Phys. Org. Chem.* **1980**, *17*, 279. (d) Cram, D. J.; Trueblood, K. N. *Top. Curr. Chem.* **1981**, *98*, 43. (d) Sutherland, I. O. *Chem. Soc. Rev.* **1986**, *15*, 63. (e) Stoddart, J. F. *Top. Stereochem.* **1987**, *17*, 205. (f) Izatt, R. M.; Wang, T.; Hathaway, J. K.; Zhang, X. X.; Curtis, J. C.; Bradshaw, J. S.; Zhu, C. Y.; Huszthy, P. *J. Inclusion Phenom.* **1994**, *17*, 157.

(20) (a) Yamaguchi, N.; Hamilton, L. M.; Gibson, H. W *Angew. Chem., Int. Ed.* **1998**, *37*, 3275. (b) Ishow, E.; Credi, A.; Balzani, V.; Spadola, F.; Mandolini, L. *Chem. Eur. J.* **1999**, *5*, 984. (c) Bryant, W. S.; Guzei, I. A.; Rheingold, A. L.; Gibson, H. W *Org. Lett.* **1999**, *1*, 47. (d) Meillon, J. C.; Voyer, N.; Biron, E.; Sanschagrin, F.; Stoddart, J. F *Angew. Chem., Int. Ed.* **2000**, *39*, 143. (e) Ashton, P. R.; Campbell, P. J.; Chrystal, E. J. T.; Glink, P. T.; Menzer, S.; Philip, D.; Spencer, N.; Stoddart, J. F.; Tasker, P. A.; Williams, D. J. *Angew. Chem., Int. Ed.* **1995**, *34*, 1869. (f) Aricó, F.; Badjić, J. D.; Cantrill, S. J.; Flood, A. H.; Leung, K. C.-F.; Liu, Y.; Stoddart, J. F. *Top. Curr. Chem.* **2005**, *279*, 203.

(21) (a) Ashton, P. R.; Campbell, P. J.; Chrystal, E. J. T.; Glink, P. T.; Menzer, S.; Philp, D.; Spencer, N.; Stoddart, J. F.; Tasker, P. A.; Williams, D. J. *Angew. Chem., Int. Ed.* **1995**, *34*, 1865. (b) Metcalfe, J. C.; Stoddart, J. F.; Jones, G. *J. Am. Chem. Soc.* **1977**, *99*, 8317. (c) Krane, J.; Aune, O. *Acta Chem. Scand. Ser. B* **1980**, *34*, 397. (d) Metcalfe, J. C.; Stoddart, J. F.; Jones, G.; Atkinson, A.; Kerr, I. S.; Williams, D. J. *J. Chem. Soc., Chem. Commun.* **1980**, 540. (e) Abed-Ali, S. S.; Brisdon, B. J.; England, R. *J. Chem. Soc., Chem. Commun.* **1987**, 1565.
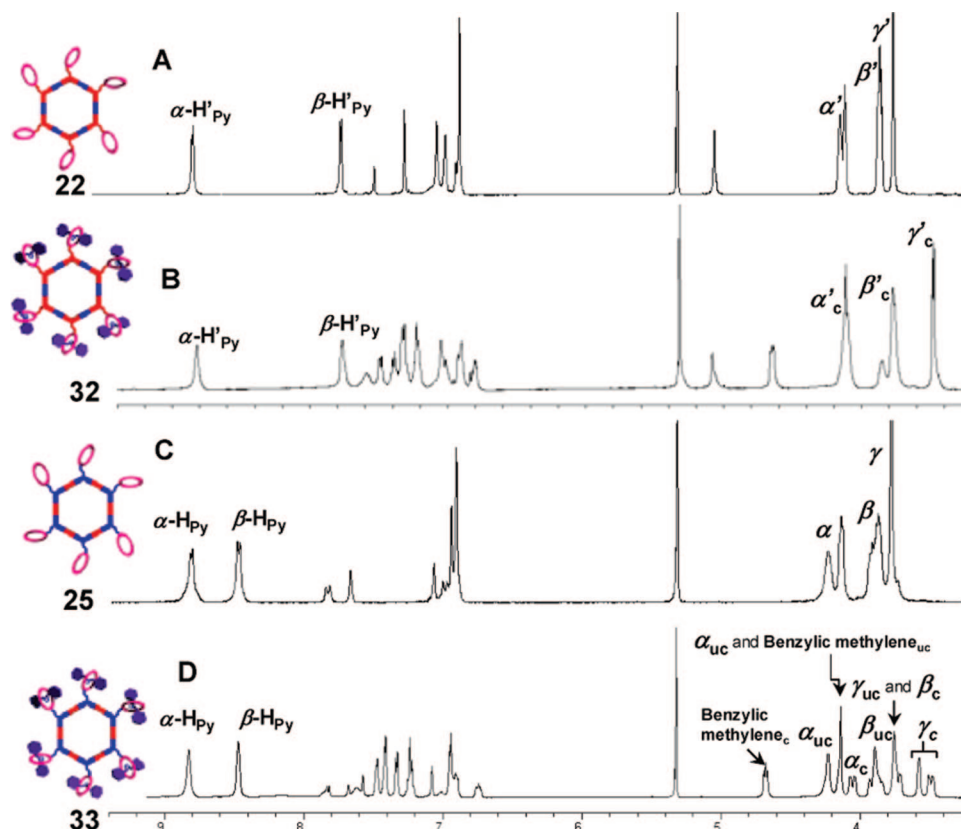
Figure 9. Partial ^{1}H NMR spectra (500 MHz, CD$_2$Cl$_2$, 298 K) of free hosts **22** (A) and **25** (C) and hexagonal hexakis[2]pseudorotaxanes **32** (B) and **33** (D).

NOESY) provided further evidence for the formation of the new hexagonal tris[2]pseudorotaxane in solution (see Supporting Information).

The highly efficient coordination-driven self-assembly of multiple crown ether derivatives, particularly of hexakis-**DB24C8** derivatives, provides the possibility of forming higher-order [2]pseudorotaxanes such as hexakis[2]pseudorotaxanes. Reports of such well-defined higher-order pseudorotaxanes have, to date, proven rare. Hexakis-**DB24C8** derivatives **22** and **25** with different sized hexagonal cavities were selected as hosts to incorporate six dibenzylammonium guests each, thus generating (Scheme 8) two different hexakis[2]pseudorotaxanes (**32** and **33**, respectively). The ^{1}H NMR spectra of a 1:6 mixture of host **22** (4.02 mmol) or **25** (4.13 mmol) and dibenzylammonium salt **26** in dichloromethane exhibited characteristic shifts associated with the complexation of dibenzylammonium ions by **DB24C8**, analogous to those that have previously been observed in the ^{1}H NMR spectra of poly[2]pseudorotaxanes **27–29**. Hexakis[2]pseudorotaxane **32** was found to be the main species in solution, as indicated (Figure 9B) by one dominant set of proton signals observed in the ^{1}H NMR spectrum. Similar to pseudorotaxanes **27** and **29**, the generation of hexakis[2]pseudorotaxane **33** results in a nearly 1:1 equilibrium mixture of complexed and uncomplexed species (Figure 9D) because of the electron-deficient nature of di-Pt(II)-linked **DB24C8** rings. Further characterization with 2-D spectroscopic techniques (^{1}H–^{1}H COSY and NOESY) supports the formation of hexagonal cavity-cored hexakis[2]pseudorotaxanes **32** and **33**. The NOESY spectrum of each complex, for example, clearly showed through-space interactions between the α-H protons of the complexed crown ether derivatives and the benzylic methylene protons (see Supporting Information). It is important to note

that the collective ^{1}H NMR spectroscopic results are able to demonstrate the orthogonality of self-assembly along this stepwise approach to **27–29**, **32**, and **33**: only those signals associated with the pyridyl functionalities of **7**, **12**, **14**, **22**, and **25** shift upon metal coordination, while only those signals associated with the derivatized **DB24C8** macrocycles shift upon complexation of **26**.

Pseudorotaxane Stoichiometry and Thermodynamics. The host:guest stoichiometry for supramolecular assemblies **27–29**, **32**, and **33** was established using the nonlinear least-squares fit method[22] based on ^{1}H NMR titration experiments (Figure 10, also see Supporting Information). Results of these studies indicate a 1:2 host:guest stoichiometry for both rhomboidal bis-**DB24C8** hosts **7** and **12**; a 1:3 host:guest stoichiometry for hexagonal tris-**DB24C8** host **14**; and a 1:6 host:guest stoichiometry for both hexakis-**DB24C8** hosts **22** and **25**, with the guest in each case being dibenzylammonium salt **26**. The stoichiometric calculations further support the formation of rhomboidal bis[2]pseudorotaxanes **27** and **28**, hexagonal tris[2]pseudorotaxane **29**, and hexagonal hexakis[2]pseudorotaxanes **32** and **33**. Fitting the data to a 1:2 binding mode for hosts **7** and **12**, a 1:3 binding mode for host **14**, and a 1:6 binding model for hosts **22** and **25** gave rise to host–guest association constants based on the ^{1}H NMR titration experiments (see Table 1). These values suggest that all multiple crown ether derivatives have an ability to bind dibenzylammonium guest(s) similar to that of **DB24C8** in a nonpolar solvent such as dichloromethane. The difference of the binding ability of each polygonal host could be determined from these values as well. In all cases, the covalent attachment of derivatized crown ether macrocycles to

(22) Bourson, J.; Pouget, J.; Valeur, B. *J. Phys. Chem.* **1993**, *97*, 4552.
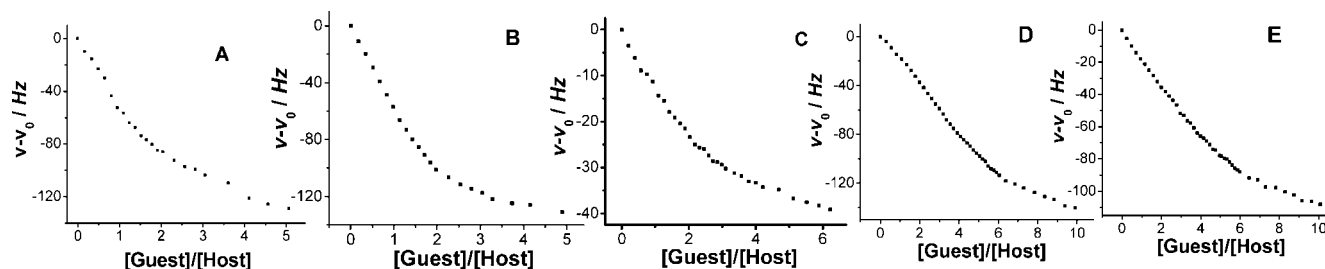
Figure 10. ^{1}H NMR titration isotherms of **27** (A), **28** (B), **29** (C), **32** (D), and **33** (E), recorded at 500 MHz in CD$_2$Cl$_2$ at 298 K (■ indicates the change in chemical shift of the proton signal corresponding to the γ-H of the crown ether).

Table 1. Thermodynamic Binding Constants (CD$_2$Cl$_2$, 298 K) of Poly[2]pseudorotaxanes **27**−**29**, **32**, and **33**

	$K_{s.1}$ (M^{-1})	$K_{s.2}$ (M^{-1})	$K_{s.3}$ (M^{-1})
27	$(1.09 \pm 0.17) \times 10^4$	$(4.55 \pm 0.04) \times 10^2$	
28	$(2.52 \pm 0.24) \times 10^4$	$(2.62 \pm 0.00) \times 10^3$	
29	$(4.89 \pm 0.63) \times 10^3$	$(1.76 \pm 0.05) \times 10^3$	$(1.06 \pm 0.01) \times 10^3$
32^a	$(1.81 \pm 0.34) \times 10^4$	$(1.20 \pm 0.13) \times 10^3$	$(5.66 \pm 0.32) \times 10^2$
33^a	$(2.06 \pm 0.10) \times 10^3$	$(9.03 \pm 0.23) \times 10^2$	$(5.39 \pm 0.03) \times 10^2$

^{a} As a result of limitations in the method of analysis used to evaluate the data obtained from ^{1}H NMR titration experiments, only $K_{s.1}$, $K_{s.2}$, and $K_{s.3}$ of **32** and **33** could be established.

di-Pt(II) building blocks results in a decreased binding ability of the resultant rhomboidal and hexagonal multi-crown ether hosts (Table 1). The decrease in $K_{s.1}$ ranges from roughly one-half in the comparison of bis-**DB24C8** rhomboids **27** and **28** up to an order of magnitude in the case of hexakis-**DB24C8** hosts **32** and **33**. These findings support the conclusion that placement of the derivatized crown ether macrocycles on acceptor building blocks results in a loss of electron density and, thus, binding ability. It can also be observed from Table 1 that, in all cases, binding constants get progressively smaller with each successive complexation of a dibenzylammonium guest. From the ratios of binding constants, it is clear that the crown ether sites act more or less independent of each other and pseudorotaxane formation is not influenced by any sort of cooperative effects.[23] Rather, the decrease in efficiency of the threading process may be attributed to the entropic cost of forming higher-order pseudorotaxanes.

Molecular force-field simulations were used to gain further insight into the structural characteristics of cavity-cored poly[2]pseudorotaxanes **27**–**29**, **32**, and **33**. A 1.0 ns molecular dynamics simulation (MMFF) was used to equilibrate each supramolecule **27**–**29**, **32**, and **33**, followed by energy minimization of the resulting structures to full convergence. The modeled structure of hexakis[2]pseudorotaxane **32**, for example, is shown in Figure 11 (for compounds **27**–**29** and **33**, see Supporting Information). Molecular simulations reveal that the addition of dibenzylammonium to **DB24C8** hosts does not disrupt the underlying polygonal scaffolds, as ammonium salts are complexed by their pendant **DB24C8** macrocycles, further illustrating the orthogonality of the noncovalent interactions involved in self-assembly. In all cases, the underlying rigid nature of the 2-D polygonal cavity is retained, while the flexibility of each crown ether is reduced as a result of host–guest complexation.
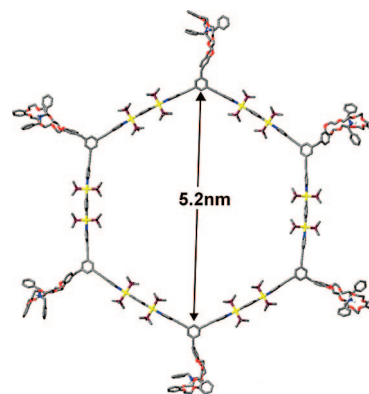
(23) Gibson, H. W.; Yamaguchi, N.; Hamilton, L.; Jones, J. W. *J. Am. Chem. Soc.* **2002**, *124*, 4653.

Figure 11. Simulated molecular model of hexagonal hexakis-**DB24C8** derivative **32**, optimized with the molecular mechanics force field. Color scheme: C, gray; O, red; N, blue; P, purple; Pt, yellow; and R$_2$NH$_2^+$ hydrogen atoms, white (all other hydrogen atoms have been removed for clarity).

Conclusions

The work presented here provides a simple, yet highly efficient approach to the construction, via coordination-driven self-assembly, of crown ether-derivatized 2-D polygons possessing structurally well-defined cavities of varying diameter and shape. The covalent attachment of a **DB24C8** macrocycle to both 120° di-Pt(II) acceptor and 120° bispyridyl donor units allows for a series of rhomboidal bis-, hexagonal tris-, and hexagonal hexakis-**DB24C8** derivatives to be self-assembled under mild conditions and in quantitative yields when combined with complementary 60°, 120°, and 180° building blocks, respectively. The resultant multi-crown ether assemblies are unique in that the number and arrangement of their pendant macrocycles can be precisely controlled owing to the conserved rigidity of their core 2-D polygonal scaffolds. Furthermore, the orthogonal, non-interacting nature of coordination-driven self-assembly of the underlying polygons and the hydrogen-bonding/electrostatic/π−π stacking-promoted self-assembly of crown ether−dialkylammonium pseudorotaxanes allows for rhomboidal and hexagonal poly[2]pseudorotaxanes to be prepared.

The facile construction of rhomboidal bis[2]pseudorotaxanes and hexagonal tris- and hexakis[2]pseudorotaxanes by this orthogonal approach not only expands upon the traditional techniques of supramolecular chemistry, where the majority of known supramolecular structures have been prepared using a single recognition motif, but also provides a new methodology to build supramolecular structures in which a variety of noncovalent interactions allow for multiple complementary components to self-assemble into supramolecular species with complex functional architectures. The demonstration of the power and scope of the orthogonal approach to supramolecular

assemblies provides a solid foundation upon which to extend these studies. It quickly becomes apparent that there are many avenues to be explored by expanding upon the orthogonal self-assembly approach, given the many 2-D and 3-D supramolecular assemblies that can be prepared, the variety of orthogonal noncovalent interactions that can be combined, and the possibility of using three or more independent, non-interacting self-assembly protocols as opposed to only two. Investigations aimed at expanding the orthogonal approach along these lines are currently underway.

Experimental Section

Triethylamine was distilled from sodium hydroxide, and tetrahydrofuran (THF) was distilled from K(s)/benzophenone. Deuterated solvents were purchased from Cambridge Isotope Laboratory (Andover, MA). All other reagents were purchased (Aldrich or Acros) and used without further purification. NMR spectra were recorded on a Varian Unity instrument (300 and 500 MHz). The ^1H and ^{13}C NMR chemical shifts are reported relative to residual solvent signals, and ^{31}P NMR resonances are referenced to an external unlocked sample of 85% H_3PO_4 (δ 0.0). Element analysis was performed in Atlantic Microlab (Norcross, GA). Mass spectra were recorded on a Micromass Quattro II triple-quadrupole mass spectrometer using electrospray ionization with a MassLynx operating system or on an ESI-TOF mass spectrometer (Agilent Technologies, Santa Clara, CA). The solvent for ESI-TOF mass spectra is dichloromethane.

Titration experiments were carried out by the addition of a concentrated CD_2Cl_2 solution of the ammonium triflate salt **26** to solutions of multiple crown ether derivative hosts **7**, **12**, **14**, **22**, and **25** in CD_2Cl_2, respectively. In order to account for dilution effects, these ammonium triflate salt solutions also contained host at its initial concentration. The association constants were calculated by the Hyperquad2003 program using changes in the chemical shift of the γ-proton resonance of crown ether in the ^1H NMR spectra.[24]

The molecular structures of all multiple crown ether derivatives as well as all poly[2]pseudorotaxanes were each constructed within the input mode of the program Maestro v8.0.110[25] with the MMFF.[26] A 1.0 ns molecular dynamics simulation (0.05 fs time step) at a simulation temperature of 300 K was used to equilibrate each structure. Following each molecular dynamics simulation, a full energy minimization was used to obtain the final optimized structures.

Synthesis of 3,5-Diethynyl-phenol (2). In a 50 mL round-bottom Schlenk flask, 3,5-dibromo-phenyl ester (**1**, 0.42 g, 1.43 mmol) and 0.83 mL of (trimethylsilyl)acetylene (11.7 mmol) were dissolved in 20 mL of freshly distilled THF and 5 mL of dry triethylamine. A mixture of 0.172 g of tetrakis(triphenylphosphine)palladium (0.149 mmol) and 53 mg of cuprous iodide (0.12 mmol) was added, and the suspension was stirred for 16 h at room temperature in the absence of light. After removal of the solvent, the residue was suspended in 50 mL of diethyl ether and washed twice with 50 mL of water, and the organic phase was dried over magnesium sulfate. After filtration, the solvents were removed, and the residue was separated by column chromatography on silica gel. With a solvent mixture (hexane/acetone: 8/1), 0.43 g (80%, R_f = 0.40, hexane/acetone: 8/1) of **1a** was isolated as a white solid.

Desilylation of **1a** (0.43 g, 1.31 mmol) was achieved by stirring the compound in a NaHCO$_3$ suspension of methanol/THF/water (0.5 g of NaHCO$_3$ in 5 mL of methanol, 5 mL of THF, and 7 mL of water) for 12 h at 55 °C. The solution was carefully diluted with 20 mL of water, and the organic product was extracted with diethyl ether. Drying the ether phase over magnesium sulfate and subsequent filtration resulted in a slightly yellow oil after removal of the solvent. Column chromatography on silica gel with a solvent mixture (hexane/acetone: 3/1) yielded **2** as a white powder. Yield: 0.17 g, 95%. Mp: 88–89 °C. R_f = 0.40 (hexane/acetone: 3/1). ^1H NMR (CDCl$_3$, 300 MHz): δ 7.21 (s, 1H), 6.94 (s, 2H), 3.07 (s, 2H). ^{13}C NMR (CDCl$_3$, 75 MHz): δ 155.3, 128.8, 123.9, 119.8, 82.4, 78.2. MS (CI): *m/z* 142.0 (M$^+$).

Synthesis of Compound 3. To a solution of dibenzo[24]crown-8 carboxylic acid[27] (172 mg, 0.35 mmol) in 5 mL of anhydrous dichloromethane were added a catalytic amount (10%) of DMAP and 3,5-diethynyl-phenol (**2**, 50 mg, 0.35 mmol). DCC was then added to the reaction mixture at 0 °C, followed by stirring for 5 min at 0 °C and 10 h at room temperature. Precipitated urea was then filtered off, and the filtrate was evaporated under vacuum. The residue was taken up in 25 mL of CH$_2$Cl$_2$, washed twice with 0.5 N HCl and with saturated NaHCO$_3$ solution, and then dried over MgSO$_4$. The residue was purified by column chromatography on silica gel (DCM/hexane: 1/1) to give compound **3**. Yield: 183 mg, 85%. Mp: 70–71 °C. R_f = 0.45 (DCM/hexane: 1/1). ^1H NMR (CD$_2$Cl$_2$, 300 MHz): δ 7.80 (dd, *J* = 6.3 Hz, *J* = 2.1 Hz, 1H), 7.63 (d, *J* = 2.1 Hz, 1H), 7.51 (s, 1H), 7.34 (s, 2H), 6.89–6.94 (m, 5H), 4.18–4.22 (m, 4H, α-CH$_2$), 4.09–4.13 (m, 4H, α-CH$_2$), 3.84–3.93 (m, 8H, β-CH$_2$), 3.77–3.78 (br, 8H, γ-CH$_2$), 3.21 (s, 2H). ^{13}C NMR (CD$_2$Cl$_2$, 75 MHz): δ 164.8, 154.4, 151.4, 149.6, 149.1, 133.4, 126.7, 125.3, 124.1, 121.9, 121.8, 115.3, 114.7, 114.6, 112.7, 82.0, 79.3, 71.8, 71.7, 71.6, 70.4, 70.2, 70.0, 69.7, 69.8 MS (ESI): *m/z* 639.3 (M + Na$^+$).

Synthesis of Diiodometal Complex 4. To a 50 mL round-bottom Schlenk flask were added *trans*-diiodobis(triethylphosphine)platinum (0.80 g, 1.17 mmol) and **3** (181 mg, 0.29 mmol). Then 15 mL of toluene and 7 mL of dry diethylamine were added under nitrogen. The solution was stirred for 10 min at room temperature before 15 mg of cuprous iodide was added in one portion. After 16 h at room temperature, a small amount of diethylammonium iodide started precipitating out of solution. The solvent was removed under vacuum, the resulting yellow residue was separated by column chromatography on silica gel with a solvent mixture (DCM/acetone: 5/1), and **4** was isolated. Yield: 326 mg, 65%. Mp: 172–173 °C. R_f = 0.35 (DCM/acetone: 5/1). ^1H NMR (CD$_2$Cl$_2$, 300 MHz): δ 7.81 (s, 1H), 7.79 (s, 1H), 7.64 (s, 2H), 7.08 (s, 2H), 6.87–6.96 (m, 5H), 4.20 (br, 4H, α-CH$_2$), 4.09–4.12 (m, 4H, α-CH$_2$), 3.86–3.97 (m, 8H, β-CH$_2$), 3.77–3.78 (m, 8H, γ-CH$_2$), 2.17–2.23 (m, 24H, PCH$_2$CH$_3$), 1.10–1.21 (m, 36H, PCH$_2$CH$_3$). ^{31}P{^1H} NMR (CD$_2$Cl$_2$, 121.4 MHz): δ 9.25 (s, $^1J_{Pt-P}$ = 2312.5 Hz). ^{13}C NMR (CD$_2$Cl$_2$, 75 MHz): δ 165.3, 154.2, 151.4, 149.6, 149.0, 130.9, 130.0, 125.0, 122.6, 121.9, 121.6, 115.3, 114.7, 114.6, 112.7, 99.6, 91.9, 71.8, 71.7, 71.6, 70.4, 70.2, 70.1, 69.8, 17.6, 17.4, 17.1, 16.9, 16.7, 8.7, 8.6, 8.4. MS (ESI): *m/z* 1752.7 (M + Na$^+$). Anal. Calcd for C$_{59}$H$_{94}$I$_2$O$_{10}$P$_4$Pt$_2$: C, 40.93; H, 5.47. Found: C, 41.24; H, 5.51.

Synthesis of Bistriflate Salt 5. A 50 mL round-bottom Schlenk flask was charged with 0.30 g (0.173 mmol) of **4** and 15 mL of dichloromethane. To the solution was added 98 mg (0.381 mmol) of AgOTf at once, resulting in a yellowish precipitate of AgI. After 4 h at room temperature, the suspension was filtered through a glass fiber and the volume of the solution reduced to 5 mL. Subsequent addition of diethyl ether resulted in the precipitation of the bistriflate salt **5** as a slightly yellow crystalline powder. Yield: 276 mg, 90%. Mp: 70–71 °C. ^1H NMR (CD$_2$Cl$_2$, 500 MHz): δ 7.83 (s, 1H), 7.81 (s, 1H), 7.66 (s, 2H), 6.81–7.00 (m, 7H), 4.23 (br, 4H, α-CH$_2$), 4.15 (br, 4H, α-CH$_2$), 3.86–3.92 (m, 8H, β-CH$_2$), 3.77 (br, 8H, γ-CH$_2$), 2.02–2.07 (m, 24H, PCH$_2$CH$_3$), 1.16–1.27 (m, 36H, PCH$_2$CH$_3$). ^{31}P{^1H} NMR (CD$_2$Cl$_2$, 121.4 MHz): δ 22.7 (s, $^1J_{Pt-P}$ = 2374.2 Hz). ^{13}C NMR (CD$_2$Cl$_2$, 75 MHz): δ 165.3, 154.2, 151.4, 149.6, 149.0, 130.9, 130.0, 125.0, 122.6, 121.9, 121.6, 115.3, 114.7, 114.6, 112.7, 99.6, 91.9, 71.8, 71.7, 71.6, 70.4, 70.2, 70.1, 69.8, 17.6, 17.4, 17.1, 16.9, 16.7, 8.7, 8.6, 8.4. MS (ESI): *m/z* 1624.9

(24) *Hyperquad2003*; Protonic Software, http://www.hyperquad.co.uk.
(25) Mohamadi, F.; Richards, N. G. J.; Guida, W. C.; Liskamp, R.; Lipton, M.; Caufield, C.; Chang, G.; Hendrickson, T.; Still, W. C. *J. Comput. Chem.* **1990**, *11*, 440.
(26) Halgren, T. A. *J. Comput. Chem.* **1996**, *17*, 490.
(27) Feng, D.-J.; Li, X.-Q.; Wang, X.-Z.; Jiang, X.-K.; Li, Z.-T. *Tetrahedron* **2004**, *60*, 6137.

(M - OTf). Anal. Calcd for $C_{61}H_{94}F_6O_{16}P_4Pt_2S_2$: C, 41.26; H, 5.34. Found: C, 40.95; H, 5.12.

Preparation of Rhomboidal Bis-DB24C8 Derivatives 7, 11, and 12. Method I: To a 0.4 mL dichloromethane-d_2 solution of 120° crown ether containing di-Pt(II) acceptor **5** (5.01 mg, 0.00282 mmol) was added a 0.4 mL dichloromethane-d_2 solution of 60° donor **6** (1.07 mg, 0.00282 mmol) drop by drop with continuous stirring (10 min). The reaction mixture was stirred for another 20 min at room temperature. The solution was evaporated to dryness, and the product of bis-**DB24C8** derivative **7** was collected as a pale yellow solid. Yield: 5.84 mg, 96%. ^{1}H NMR (CD$_2$Cl$_2$, 500 MHz): δ 9.05–9.18 (m, 4H, H$_4$), 8.65 (d, J = 5.4 Hz, 8H, H$_α$-Py), 7.83–7.99 (m, 22H, H$_1$, H$_2$, H$_{10}$, Ar*H*, and H$_β$-Py), 7.66 (s, 4H, Ar*H*), 6.89–7.07 (m, 14H, Ph*H*), 4.22 (br, 8H, α-CH_2), 4.12 (br, 8H, α-CH_2), 3.85–3.90 (m, 16H, β-CH_2), 3.76 (br, 16H, γ-CH_2), 1.83 (br, 48H, PCH_2CH$_3$), 1.19 (br, 72H, PCH$_2$CH_3). ^{31}P{^{1}H} NMR (CD$_2$Cl$_2$, 121.4 MHz): δ 16.0 (s, $^1J_{Pt-P}$ = 2307.8 Hz). Anal. Calcd for $C_{178}H_{224}F_{12}N_4O_{30}P_8Pt_4S_4$: C, 49.90; H, 5.27; N, 1.31. Found: C, 49.59; H, 5.03; N, 1.22.

Method II: To a 0.5 mL dichloromethane-d_2 solution of small 60° angular Pt(II) acceptor **9** (4.50 mg, 0.00387 mmol) or large 60° angular Pt(II) acceptor **10** (5.36 mg, 0.00387 mmol), respectively was added a 0.5 mL dichloromethane-d_2 solution of 120° crown ether containing donor **8** (2.93 mg, 0.00387 mmol) drop by drop with continuous stirring (10 min). The reaction mixture was stirred overnight (for **9**) or for another 20 min (for **10**) at room temperature. The solution was evaporated to dryness, and the product of bis-**DB24C8** derivative **11** (white solid) or **12** (pale yellow solid) was collected, respectively.

11. Yield: 7.13 mg, 96%. ^{1}H NMR (CD$_2$Cl$_2$, 500 MHz): δ 9.33 (d, J = 6.0 Hz, 4H, H$_α$-Py), 8.82 (s, 4H, H$_4$), 8.70 (d, J = 6.0 Hz, 4H, H$_α$-Py), 7.96 (d, J = 5.7 Hz, 4H, H$_β$-Py), 7.79 (d, J = 5.7 Hz, 4H, H$_β$-Py), 7.65 (s, 2H, Ar*H*), 7.58–7.60 (m, 12H, H$_1$, H$_2$, and H$_{10}$), 7.37 (s, 4H, Ar*H*), 7.02–7.04 (m, 4H, Ph*H*), 6.90–6.94 (m, 10H, Ph*H*), 5.09 (s, 4H, PhCH_2O), 4.11–4.19 (m, 16H, α-CH_2), 3.85–3.91 (m, 16H, β-CH_2), 3.76–3.78 (m, 16H, γ-CH_2), 1.36–1.41 (m, 48H, PCH_2CH$_3$), 1.05–1.20 (m, 72H, PCH$_2$CH_3). ^{31}P{^{1}H} NMR (CD$_2$Cl$_2$, 121.4 MHz): δ 12.6 (s, $^1J_{Pt-P}$ = 2707.3 Hz). Anal. Calcd for $C_{166}H_{224}N_8O_{30}P_8Pt_4$: C, 51.93; H, 5.88; N, 2.92. Found: C, 51.63; H, 5.78; N, 2.96.

12. Yield: 7.79 mg, 94%. ^{1}H NMR (CD$_2$Cl$_2$, 500 MHz): δ 8.69 (d, J = 5.4 Hz, 8H, H$_α$-Py), 8.51 (s, 4H, H$_4$), 7.80–7.84 (m, 12H, H$_b$-Py and H$_1$), 7.68 (s, 4H, H$_{10}$), 7.50–7.60 (m, 6H, H$_2$ and Ar*H*), 7.34 (s, 4H, Ar*H*), 7.01 (d, 4H, Ph*H*), 6.89–6.90 (m, 10H, Ph*H*), 5.07 (s, 4H, PhCH_2O), 4.12–4.14 (m, 16H, α-CH_2), 3.85 (br, 16H, β-CH_2), 3.75–3.76 (m, 16H, γ-CH_2), 1.87 (br, 48H, PCH_2CH$_3$), 1.21–1.26 (m, 72H, PCH$_2$CH_3). ^{31}P{^{1}H} NMR (CD$_2$Cl$_2$, 121.4 MHz): δ 16.1 (s, $^1J_{Pt-P}$ = 2319.2 Hz). Anal. Calcd for $C_{178}H_{224}F_{12}N_4O_{30}P_8Pt_4S_4 \cdot CH_2Cl_2$: C, 49.21; H, 5.21; N, 1.28. Found: C, 49.01; H, 5.18; N, 1.31.

Preparation of Tris-DB24C8 Derivative 14. To a 0.65 mL CD$_2$Cl$_2$ solution of 120° crown ether-containing di-Pt(II) acceptor **5** (9.03 mg, 0.00509 mmol) was added a 0.65 mL CD$_2$Cl$_2$ solution of di-2-pyridyl ketone **13** (0.94 mg, 0.00509 mmol) drop by drop with continuous stirring (15 min). The reaction mixture was stirred for 30 min at room temperature. The solution was evaporated to dryness, and the product of tris-**DB24C8** derivative **14** was collected as a pale yellow solid. Yield: 9.57 mg, 96%. ^{1}H NMR (CD$_2$Cl$_2$, 500 MHz): δ 8.93 (d, J = 5.7 Hz, 12H, H$_α$-Py), 8.20 (d, J = 6.0 Hz, 12H, H$_β$-Py), 7.84 (s, 3H, Ar*H*), 7.81 (s, 3H, Ph*H*), 7.66 (s, 6H, Ar*H*), 6.91–7.01 (m, 18H, Ph*H*), 4.23 (br, 12H, α-CH_2), 4.12–4.15 (m, 12H, α-CH_2), 3.86–3.91 (m, 24H, β-CH_2), 3.78 (br, 24H, γ-CH_2), 1.83–1.85 (m, 72H, PCH_2CH$_3$), 1.14–1.26 (m, 108H, PCH$_2$CH_3). ^{31}P{^{1}H} NMR (CD$_2$Cl$_2$, 121.4 MHz): δ 16.0 (s, $^1J_{Pt-P}$ = 2289.5 Hz). Anal. Calcd for $C_{216}H_{306}F_{18}N_6O_{51}P_{12}Pt_6S_6$: C, 44.13; H, 5.25; N, 1.43. Found: C, 43.88; H, 5.03; N, 1.35.

Preparation of Hexakis-DB24C8 Derivatives 19, 22, 23, and 25. Method I: To a 0.40 mL CD$_2$Cl$_2$ solution of 120° crown ether-containing di-Pt(II) acceptor **5** (4.0 mg, 0.00225 mmol) was added a 0.40 mL CD$_2$Cl$_2$ solution of 120° crown ether-containing donor **8** (1.71 mg, 0.00225 mmol) drop by drop with continuous stirring (10 min). The reaction mixture was stirred for 30 min at room temperature. The solution was evaporated to dryness, and the product of hexakis-**DB24C8** derivative **19** was collected as a pale yellow solid. Yield: 5.60 mg, 98%. ^{1}H NMR (CD$_2$Cl$_2$, 500 MHz): δ 8.63 (d, J = 5.5 Hz, 12H, H$_α$-Py), 7.81–7.82 (m, 15H, H$_β$-Py and Ar*H*), 7.65 (s, 6H, Ar*H*), 7.56 (s, 3H, Ar*H*), 7.33 (br, 9H, Ar*H* and Ph*H*), 6.89–7.06 (m, 18H, Ph*H*), 5.07 (s, 6H, PhCH_2O), 4.22 (br, 12H, α-CH_2), 4.17 (br, 12H, α-CH_2), 4.12 (br, 24H, α-CH_2), 3.86–3.92 (m, 48H, β-CH_2), 3.78 (br, 24H, γ-CH_2), 3.76 (br, 24H, γ-CH_2), 1.80–1.83 (m, 72H, PCH_2CH$_3$), 1.15–1.22 (m, 108H, PCH$_2$CH_3). ^{31}P{^{1}H} NMR (CD$_2$Cl$_2$, 121.4 MHz): δ 18.3 (s, $^1J_{Pt-P}$ = 2309.5 Hz). Anal. Calcd for $C_{318}H_{414}F_{18}N_6O_{75}P_{12}Pt_6S_6 \cdot CH_2Cl_2$: C, 49.87; H, 5.46; N, 1.09. Found: C, 49.51; H, 5.33; N, 1.11.

Method II: To a 0.5 mL dichloromethane-d_2 solution of small 180° angular Pt(II) acceptor **20** (3.53 mg, 0.0033 mmol) or large 180° angular Pt(II) acceptor **21** (4.33 mg, 0.0033 mmol) was added a 0.5 mL dichloromethane-d_2 solution of 120° crown ether-containing donor **8** (2.50 mg, 0.0033 mmol) drop by drop with continuous stirring (10 min). The reaction mixture was stirred for another 20 min at room temperature. The solution was evaporated to dryness, and the product of hexakis-**DB24C8** derivative **22** (pale yellow solid) or **23** (pale yellow solid) was collected, respectively.

22. Yield: 5.85 mg, 97%. ^{1}H NMR (CD$_2$Cl$_2$, 500 MHz): δ 8.82 (d, J = 6.0 Hz, 24H, H$_α$-Py), 7.75 (d, J = 6.5 Hz, 24H, H$_β$-Py), 7.51 (s, 6H, Ar*H*), 7.29 (s, 12H, Ar*H*), 7.06 (s, 24H, Ar*H*), 6.99 (s, 12H, Ph*H*), 6.89–6.92 (m, 30H, Ph*H*), 5.05 (s, 12H, PhCH_2O), 4.11–4.16 (m, 48H, α-CH_2), 3.84–3.87 (m, 48H, β-CH_2), 3.76 (br, 48H, γ-CH_2), 1.10–1.17 (m, 216H, PCH_3). ^{31}P{^{1}H} NMR (CD$_2$Cl$_2$, 121.4 MHz): δ 14.8 (s, $^1J_{Pt-P}$ = 2731.7 Hz). Anal. Calcd for $C_{390}H_{504}F_{36}N_{12}O_{90}P_{24}Pt_{12}S_{12}$: C, 42.77; H, 4.64; N, 1.53. Found: C, 42.43; H, 4.93; N, 1.46.

23. Yield: 6.49 mg, 95%. ^{1}H NMR (CD$_2$Cl$_2$, 500 MHz): δ 8.69 (d, J = 5.5 Hz, 24H, H$_α$-Py), 7.82 (d, J = 6.6 Hz, 24H, H$_β$-Py), 7.61 (s, 6H, Ar*H*), 7.41 (br, 48H, Ar*H*), 7.33 (s, 12H, Ar*H*), 7.01 (s, 12H, Ph*H*), 6.89–6.93 (m, 30H, Ph*H*), 5.07 (s, 12H, PhCH_2O), 4.11–4.17 (m, 48H, α-CH_2), 3.85–3.89 (m, 48H, β-CH_2), 3.77–3.78 (m, 48H, γ-CH_2), 1.36–1.41 (m, 144H, PCH_2CH$_3$), 1.13–1.17 (m, 216H, PCH$_2$CH_3). ^{31}P{^{1}H} NMR (CD$_2$Cl$_2$, 121.4 MHz): δ 14.1 (s, $^1J_{Pt-P}$ = 2684.0 Hz). Anal. Calcd for $C_{490}H_{672}F_{36}N_{12}O_{90}P_{24}Pt_{12}S_{12}$: C, 48.16; H, 5.45; N, 1.35. Found: C, 48.14; H, 5.66; N, 1.28.

Method III: To a 0.60 mL CD$_2$Cl$_2$ solution of 120° crown ether-containing di-Pt(II) acceptor **5** (7.95 mg, 0.00448 mmol) was added a 0.60 mL CD$_2$Cl$_2$ solution of linear 4,4′-bipyridyl donor **24** (0.70 mg, 0.00225 mmol) drop by drop with continuous stirring (10 min). The reaction mixture was stirred for 30 min at room temperature. The solution was evaporated to dryness, and the product of hexakis-**DB24C8** derivative **25** was collected as a pale yellow solid. Yield: 8.30 mg, 96%. ^{1}H NMR (CD$_2$Cl$_2$, 500 MHz): δ 8.82 (d, J = 5.5 Hz, 24H, H$_α$-Py), 8.48 (d, J = 6.0 Hz, 24H, H$_β$-Py), 7.83 (s, 6H, Ar*H*), 7.81 (s, 6H, Ph*H*), 7.66 (s, 12H, Ar*H*), 7.07 (s, 12H, Ph*H*), 6.90–6.98 (m, 24H, Ph*H*), 4.22 (br, 24H, α-CH_2), 4.13 (br, 24H, α-CH_2), 3.86–3.92 (m, 48H, β-CH_2), 3.78 (br, 48H, γ-CH_2), 1.82–1.85 (m, 144H, PCH_2CH$_3$), 1.18–1.23 (m, 216H, PCH$_2$CH_3). ^{31}P{^{1}H} NMR (CD$_2$Cl$_2$, 121.4 MHz): δ 16.3 (s, $^1J_{Pt-P}$ = 2307.7 Hz). Anal. Calcd for $C_{426}H_{612}F_{36}N_{12}O_{96}P_{24}Pt_{12}S_{12}$: C, 44.14; H, 5.32; N, 1.45. Found: C, 44.02; H, 5.21; N, 1.36.

Supporting Information Available: ^{1}H and ^{13}C NMR spectra of compounds **2–4**, ^{1}H and ^{31}P NMR spectra of **5**, **7**, **11**, **12**, **14**, **19**, **22**, **23**, **25**, **27–29**, **32**, and **33**, and two-dimensional spectra (^{1}H−^{1}H COSY and NOESY) of **27–29**, **32**, and **33**; experimental data for ^{1}H NMR titration experiments; and computational procedures and structures for all self-assemblies obtained from modeling. This material is available free of charge via the Internet at http://pubs.acs.org.

JA711502T